FACULTY OF BUSINESS & ECONOMICS

THE UNIVERSITY OF MELBOURNE

Melbourne Institute Working Paper Series

Working Paper No. 4/16

Risk and Return Spillovers among the G10 Currencies

Matthew Greenwood-Nimmo, Viet Hoang Nguyen and Barry Rafferty

MELBOURNE INSTITUTE®
of Applied Economic and Social Research

Risk and Return Spillovers among the G10 Currencies*

Matthew Greenwood-Nimmo†, Viet Hoang Nguyen‡ and Barry Rafferty†

† Department of Economics, The University of Melbourne

‡ Melbourne Institute of Applied Economic and Social Research, The University of Melbourne

Melbourne Institute Working Paper No. 4/16

ISSN 1328-4991 (Print)

ISSN 1447-5863 (Online)

ISBN 978-0-7340-4402-0

February 2016

* We are indebted to J.P. Morgan and to Raphael Brun-Aguerre in particular for providing the FX options data used to compute the risk-neutral moments. We have benefited from constructive discussions with Heather Anderson, Alessio Bonato, Efrem Castelnuovo, Yu-chin Chen, Vance Martin, Anella Munro, Chris Neely, Kalvinder Shields, Yongcheol Shin and Chris Skeels and from the comments of participants at the First Conference on Recent Developments in Financial Econometrics and Applications (Deakin University, December 2014) and at a research seminar at the University of Auckland. Financial support from the Faculty of Business and Economics at the University of Melbourne is gratefully acknowledged. The usual disclaimer applies. For correspondence, email <barry.rafferty@ unimelb.edu.au>.

Melbourne Institute of Applied Economic and Social Research

The University of Melbourne

Victoria 3010 Australia

***Telephone* (03) 8344 2100**

***Fax* (03) 8344 2111**

***Email* melb-inst@unimelb.edu.au**

***WWW Address* http://www.melbourneinstitute.com**

Abstract

We study spillovers among daily returns and innovations in option-implied risk-neutral volatility and skewness of the G10 currencies. An empirical network model uncovers substantial time variation in the interaction of risk measures and returns, both within and between currencies. We find that aggregate spillover intensity is countercyclical with respect to the federal funds rate and increases in periods of financial stress. During these times, volatility spillovers and especially skewness spillovers between currencies increase, reflecting greater systematic risk. Likewise, linkages between returns and risk measures strengthen in times of stress, with returns becoming more sensitive to risk measures and vice versa.

JEL classification: C58, F31, G01, G15

Keywords: Foreign exchange markets, risk-neutral volatility, risk-neutral skewness, spillovers, coordinated crash risk

1. Introduction

To what extent are currency markets connected to one-another? This is a central question facing foreign exchange (FX) investors as they form and manage portfolios conditional on the risk-return profiles of a basket of currencies, typically seeking to manage their exposure to idiosyncratic risk through diversification. Changes in currencies' risk-return profiles will often induce portfolio rebalancing. However, in the act of rebalancing, investors' collective actions are likely to further change the risk-return profiles. This feedback effect will induce a complex array of interactions — or spillovers — among currency returns and a variety of risk measures, both within and between currency markets. Network analysis provides a natural framework to study such complex dynamic phenomena (Diebold and Yilmaz, 2009, 2014; Billio, Getmansky, Lo, and Pelizzon, 2012). However, network models remain scarce in the FX literature. We therefore develop an empirical network model to study risk and return spillovers within and between the major global currencies.

Given the importance of portfolio rebalancing in the network dynamics of FX markets, our model has two salient features. First, since FX portfolios are typically composed of several currencies, we work with a comprehensive panel dataset covering the G10 currencies. These currencies are among the world's most actively traded and liquid, collectively accounting for the large majority of turnover in global FX markets[1]. This extensive cross-sectional coverage of FX markets allows us to capture the large majority of investors' rebalancing activities. Second, to account for the different types of risk that currency investors face, we follow the emphasis in the FX asset pricing literature and include both the volatility and the skewness of changes in the exchange rate within our model. Specifically, since portfolio rebalancing is forward-looking, our analysis is based on forward-looking measures of volatility and skewness extracted from FX options data.

Volatility has long been used as a measure of uncertainty and a sophisticated literature has documented the linkage between returns and volatility. For example, Menkhoff, Sarno, Schmeling, and Schrimpf (2012) show that differences in exposure to innovations in an aggregate measure of global FX volatility play an important role in explaining the cross-sectional differences in the average excess returns of interest rate sorted currency portfolios and, therefore, in the average

[1]This can be clearly seen in the triennial survey of turnover in foreign exchange markets published by the Bank for International Settlements, the most recent of which is available at http://www.bis.org/publ/rpfx13fx.pdf.

excess return to the carry trade strategy. Changes in global FX volatility have also been shown to help to predict carry trade returns in the time series dimension by Bakshi and Panayotov (2013).

Skewness, meanwhile, measures 'crash risk', the risk associated with large jumps or crashes in the exchange rate, whether depreciations or appreciations. Crash risk has gained prominence as a factor underlying the high average excess returns to various currency strategies. A negative cross-sectional relationship between interest rate differentials and currency skewness has been documented at the individual currency level by Brunnermeier, Nagel, and Pedersen (2009) and Jurek (2014). Furthermore, Rafferty (2012) demonstrates that exposure to a global FX skewness measure explains a large proportion of the high average excess returns not just to the carry trade but also to currency momentum and value strategies. Rafferty's approach captures the risk of a *coordinated crash*, in which high yield investment currencies sharply depreciate and low yield funding currencies simultaneously appreciate. Coordinated crashes were observed during the global financial crisis (GFC), as funding liquidity constraints led to the sudden unwinding of carry trades.[2]

Our use of option-implied volatility and skewness accords with recent developments in the literature and confers several significant benefits relative to the use of latent or realised measures of volatility and skewness (Christoffersen, Jacobs, and Chang, 2013; Chang, Christoffersen, and Jacobs, 2013; Conrad, Dittmar, and Ghysels, 2013). Since they are computed every day using one day of options prices, our option-implied series provide truly conditional market-based estimates of the risk-neutral expected volatility and skewness that investors anticipate over the option maturity. As such, the option-implied measures capture investors' beliefs and risk preferences in a forward-looking manner which reflects ex ante measures of expected volatility and skewness.

To recover the moments of the option-implied (risk-neutral) distribution of future exchange rate changes, we use the model-free methodology of Bakshi and Madan (2000), Carr and Madan (2001) and Bakshi, Kapadia, and Madan (2003).[3] In this way, we construct daily option-implied measures of volatility and skewness for each of the G10 currencies against the U.S. dollar over the

[2]Another branch of the literature evaluates the importance of crash risk by comparing the returns to unhedged versus option-hedged carry trades (e.g. Burnside, Eichenbaum, Kleshchelski, and Rebelo, 2011; Jurek, 2014). The results indicate that much of the average excess return to the carry trade may be attributed to crash risk.

[3]A sizeable literature has studied the role of option-implied volatility and skewness in asset pricing, particularly with respect to equity markets (Ang, Hodrick, Xing, and Zhang, 2006, 2009; Chang et al., 2013; Conrad et al., 2013). A growing literature has applied similar techniques to the FX markets (Chen and Gwati, 2014; Jurek, 2014).

period January 1999 to October 2014 using a rich dataset of FX options prices obtained from J.P. Morgan. To account for the autocorrelation structure of the risk-neutral moments, we follow the precedent established by Menkhoff et al. (2012) and Chang et al. (2013) in the equity literature and extract the innovations in the risk-neutral volatility (RNV) and skewness (RNS) of exchange rate changes based on auxiliary first order autoregressions.

Our empirical results are derived from a generalisation of the connectedness framework developed by Diebold and Yilmaz (2009, 2014), in which one infers the structure of a network based on forecast error variance decomposition of an underlying vector autoregression. The generalisation that we employ is due to Greenwood-Nimmo, Nguyen, and Shin (2015a), whose method accommodates arbitrary aggregations of the connectedness matrix. The benefit of this approach is that it provides a means to transform the connectedness matrix to directly capture connectedness among groups of variables (e.g. among currency markets, where we observe the return, RNV and RNS innovations for each market) as opposed to connectedness among individual variables.

Our analysis proceeds in two parts. First, we establish a benchmark by evaluating the connectedness among currencies over the full sample period, from January 1999 to October 2014. This reveals significant spillovers among returns, with particularly strong bilateral spillovers among currencies that share an underlying linkage, including the European currencies and also the commodity currencies. Spillovers of RNV innovations across currencies exert a strong influence over the evolution of volatility in each market, accounting for as much as 75% of the ten-days-ahead forecast error variance of RNV innovations. By contrast, currency-specific or idiosyncratic factors strongly influence the behaviour of RNS innovations, reflecting the importance of market-specific shocks in driving the risk of large jumps or crashes in exchange rates.

Next, we analyse time variation in the pattern and intensity of spillovers using rolling samples of 250 trading days. This reveals that aggregate spillover intensity is inversely related to the federal funds rate, indicating that spillovers strengthen (weaken) as economic and financial conditions in the U.S. deteriorate (improve). Similarly, spillovers intensify during periods of illiquidity (captured via the TED spread) and periods of uncertainty in equity markets (represented by the VIX). Adverse shocks — particularly the GFC and the European sovereign debt crisis — are associated with a marked increase in spillover intensity. Spillovers from RNV and RNS innovations to realised returns pick up substantially during the crises as investors strive to manage their risk exposure through portfolio rebalancing. Cross-market skewness spillovers intensify particularly markedly at this time, reflecting a sharp increase in coordinated crash risk, a finding which reflects the well-documented liquidity constraints that emerged during the crises.

Our paper is a logical development of the literature on volatility spillovers initiated by Engle, Ito, and Lin (1990). The early papers in this literature use GARCH-type models to construct latent measures of volatility (e.g. Kearney and Patton, 2000; Hong, 2001). More recently, the focus has shifted towards the use of high-frequency realised volatility measures (e.g. Melvin and Melvin, 2003; Cai, Howorka, and Wongswan, 2008; Bubák, Kočenda, and Žikeš, 2011). We are aware of just one study which uses option-implied volatilities. Nikkinen, Sahlström, and Vähämaa (2006) work with option-implied volatilities derived from the Garman and Kohlhagen (1983) model to study volatility transmission in three currency pairs using just two years of data. None of these studies employ a network model or account for the interaction of returns with higher-order moments. Consequently, our work significantly extends the frontier demarcated by the existing literature.

This paper proceeds as follows. Section 2 outlines our empirical methodology. Section 3 discusses our dataset, including the computation of the moments of the risk-neutral distribution of expected exchange rate changes. Sections 4–6 present our main findings and several robustness exercises. Section 7 concludes. Additional details are provided in an online Technical Supplement.

2. Empirical Framework

2.1. The Model

We consider the bilateral exchange rates for $i = 1, 2, \ldots, N$ currencies quoted against the U.S. dollar at daily frequency over $t = 1, 2, \ldots, T$ trading days. For each currency, we observe the return, r_{it}, the innovation in risk-neutral volatility, v_{it} and the innovation in risk-neutral skewness, s_{it}. Section 3 contains detailed definitions of these variables. The 3×1 vector $\boldsymbol{y}_{it} = (r_{it}, v_{it}, s_{it})'$ collects the market-specific variables for the i-th market and the $3N \times 1$ vector $\boldsymbol{y}_t = (\boldsymbol{y}'_{1t}, \boldsymbol{y}'_{2t}, \ldots, \boldsymbol{y}'_{Nt})'$ contains all variables for every market. The total number of variables in the system is $d = 3N$.

Given our opening premise that ongoing rebalancing activity leads to complex feedback effects within and between FX markets, we require an approximating model which allows all variables to be endogenously determined. A finite order VAR is a leading candidate (Diebold and Yilmaz, 2014). Abstracting from deterministic terms for clarity of exposition, the p-th order reduced form vector autoregression for the $d \times 1$ vector of variables $\boldsymbol{y}_t$ may be written as follows:

$$\boldsymbol{y}_t = \sum_{j=1}^{p} \boldsymbol{A}_j \boldsymbol{y}_{t-j} + \boldsymbol{u}_t \tag{1}$$

where the $\boldsymbol{A}_j$'s are $d \times d$ coefficient matrices and $\boldsymbol{u}_t \sim N(\boldsymbol{0}, \boldsymbol{\Sigma}_u)$ contains the reduced form residuals, which have covariance matrix $\boldsymbol{\Sigma}_u$. Pesaran and Shin (1998) show that the h-step-ahead generalised forecast error variance decomposition (GVD) for the i-th variable is given by:

$$\vartheta_{i \leftarrow j}^{(h)} = \frac{\sigma_{u,jj}^{-1} \sum_{\ell=0}^{h-1} \left(\boldsymbol{\epsilon}_i' \boldsymbol{B}_\ell \boldsymbol{\Sigma}_u \boldsymbol{\epsilon}_j\right)^2}{\sum_{\ell=0}^{h-1} \boldsymbol{\epsilon}_i' \boldsymbol{B}_\ell \boldsymbol{\Sigma}_u \boldsymbol{B}_\ell' \boldsymbol{\epsilon}_i} \tag{2}$$

for $i, j = 1, \ldots, d$, where $\sigma_{u,jj}$ is the jth diagonal element of $\boldsymbol{\Sigma}_u$, $\boldsymbol{\epsilon}_i$ is a $d \times 1$ selection vector with its i-th element set to unity and zeros elsewhere and where the $\boldsymbol{B}_\ell$'s are the parameters of the infinite order moving average representation of the VAR which are defined recursively as $\boldsymbol{B}_\ell = \boldsymbol{A}_1 \boldsymbol{B}_{\ell-1} + \boldsymbol{A}_2 \boldsymbol{B}_{\ell-2} + \ldots$ for $\ell = 1, 2, \ldots$ with $\boldsymbol{B}_0 = \boldsymbol{I}_d$ and $\boldsymbol{B}_\ell = \boldsymbol{0}$ for $\ell < 0$. $\vartheta_{i \leftarrow j}^{(h)}$ expresses the proportion of the h-step-ahead forecast error variance (FEV) of variable i which can be attributed to shocks in the equation for variable j. GVDs have the benefit of order invariance, although it will generally be the case that $\sum_{j=1}^{d} \vartheta_{i \leftarrow j}^{(h)} > 1$ due to the non-zero correlation between reduced form shocks. Following Diebold and Yilmaz (2014), the percentage interpretation of the FEV shares can be restored by normalising such that $\theta_{i \leftarrow j}^{(h)} = 100 \times \left(\vartheta_{i \leftarrow j}^{(h)} / \sum_{j=1}^{d} \vartheta_{i \leftarrow j}^{(h)}\right) \%$.

2.2. Measuring Connectedness using VAR Models

Our goal in developing a network model is to estimate an adjacency matrix summarising the linkages (edges) among nodes in the network. The adjacency matrix for a d-variable system is a $d \times d$ matrix $\boldsymbol{C}$ whose (i, j)-th element, c_{ij}, is non-zero only if there is a linkage from node j to node i. Ex ante, it is reasonable to believe that each FX market is connected to every other and that each element of $\boldsymbol{C}$ will be non-zero. Our task is then simply to estimate the strength (weight) of each linkage in the network. Also, with no reason to presume that linkages among FX markets are symmetric, we must estimate a directed network, allowing $\boldsymbol{C}$ to be asymmetric.

An elegant framework to estimate an adjacency matrix for a weighted directed network has been proposed by Diebold and Yilmaz (2009, 2014). Their key innovation is to estimate the adjacency matrix using forecast error variance decompositions applied to an underlying VAR model. They construct the h-step-ahead $d \times d$ connectedness matrix among the d variables in $\boldsymbol{y}_t$ as follows:

$$\mathbb{C}^{(h)} = \begin{bmatrix} \theta^{(h)}_{1\leftarrow 1} & \theta^{(h)}_{1\leftarrow 2} & \cdots & \theta^{(h)}_{1\leftarrow d} \\ \theta^{(h)}_{2\leftarrow 1} & \theta^{(h)}_{2\leftarrow 2} & \cdots & \theta^{(h)}_{2\leftarrow d} \\ \vdots & \vdots & \ddots & \vdots \\ \theta^{(h)}_{d\leftarrow 1} & \theta^{(h)}_{d\leftarrow 2} & \cdots & \theta^{(h)}_{d\leftarrow d} \end{bmatrix} \tag{3}$$

Diebold and Yilmaz show that $\theta^{(h)}_{i\leftarrow j}$ measures the pairwise spillover from variable j to variable i. Furthermore — and importantly in our context — this is a directional measure because it will generally be the case that $\theta^{(h)}_{i\leftarrow j} \neq \theta^{(h)}_{j\leftarrow i}$. We may now define the following:

$$O^{(h)}_{i\leftarrow i} = \theta^{(h)}_{i\leftarrow i} \;\; ; \;\; F^{(h)}_{i\leftarrow \bullet} = \sum_{j=1, j\neq i}^{d} \theta^{(h)}_{i\leftarrow j} \;\; \text{and} \;\; T^{(h)}_{\bullet\leftarrow i} = \sum_{j=1, j\neq i}^{d} \theta^{(h)}_{j\leftarrow i} \; . \tag{4}$$

The proportion of the h-step-ahead FEV of the i-th variable that can be attributed to shocks to variable i itself is known as the *own variance share*, $O^{(h)}_{i\leftarrow i}$. The total spillovers from the system to variable i are given by $F^{(h)}_{i\leftarrow \bullet}$, which is referred to as the *from* connectedness of variable i. Likewise, the total spillovers from variable i to the system are measured by $T^{(h)}_{\bullet\leftarrow i}$, which is referred to as the *to* connectedness of variable i. It follows that $O^{(h)}_{i\leftarrow i} + F^{(h)}_{i\leftarrow \bullet} = 100\%$ by construction but that $T^{(h)}_{\bullet\leftarrow i}$ may exceed 100%. Finally, we define the following aggregate summary measures:

$$S^{(h)} = \frac{1}{d} \sum_{i=1}^{d} F^{(h)}_{i\leftarrow \bullet} \quad \text{and} \quad H^{(h)} = 100 - S^{(h)} \tag{5}$$

where $S^{(h)}$ denotes the aggregate spillover index and $H^{(h)}$ is the aggregate own-variable effect.

2.3. Block Aggregation of the Connectedness Matrix

The Diebold-Yilmaz framework can be used either to measure spillovers among individual variables or to summarise aggregate spillover activity among all variables in the system being studied. However, it does not provide a simple way to measure spillovers among *groups* of variables. As such, it is not straightforward to measure spillovers among multiple markets, each of which is represented by the three variables: r_{it}, v_{it} and s_{it}. Consequently, Greenwood-Nimmo et al. (2015a) develop a generalised framework which exploits block aggregation of the connectedness matrix.

Block aggregation introduces a new stratum between the level of individual variables and the systemwide aggregate level, thereby enhancing the flexibility of the Diebold-Yilmaz framework.

Suppose that the variables are in the order $\boldsymbol{y}_t = (r_{1t}, v_{1t}, s_{1t}, r_{2t}, v_{2t}, s_{2t}, \ldots, r_{Nt}, v_{Nt}, s_{Nt})'$ and that we wish to evaluate the connectedness among the N markets in the model in a combined manner that encompasses all three variables in each market. We may write the connectedness matrix $\mathbb{C}^{(h)}$ in block form with $g = N$ groups each composed of $m = 3$ variables as follows:

$$\mathbb{C}^{(h)} = \begin{bmatrix} \mathbf{B}^{(h)}_{1\leftarrow 1} & \mathbf{B}^{(h)}_{1\leftarrow 2} & \cdots & \mathbf{B}^{(h)}_{1\leftarrow N} \\ \mathbf{B}^{(h)}_{2\leftarrow 1} & \mathbf{B}^{(h)}_{2\leftarrow 2} & \cdots & \mathbf{B}^{(h)}_{2\leftarrow N} \\ \vdots & \vdots & \ddots & \vdots \\ \mathbf{B}^{(h)}_{N\leftarrow 1} & \mathbf{B}^{(h)}_{N\leftarrow 2} & \cdots & \mathbf{B}^{(h)}_{N\leftarrow N} \end{bmatrix}, \quad \mathbf{B}^{(h)}_{i\leftarrow j} = \begin{bmatrix} \theta^{(h)}_{r_i\leftarrow r_j} & \theta^{(h)}_{r_i\leftarrow v_j} & \theta^{(h)}_{r_i\leftarrow s_j} \\ \theta^{(h)}_{v_i\leftarrow r_j} & \theta^{(h)}_{v_i\leftarrow v_j} & \theta^{(h)}_{v_i\leftarrow s_j} \\ \theta^{(h)}_{s_i\leftarrow r_j} & \theta^{(h)}_{s_i\leftarrow v_j} & \theta^{(h)}_{s_i\leftarrow s_j} \end{bmatrix} \quad (6)$$

for $i, j = 1, 2, \ldots, N$ and where the block $\mathbf{B}^{(h)}_{i\leftarrow i}$ collects all the within-market effects for market i while $\mathbf{B}^{(h)}_{i\leftarrow j}$ collects all spillover effects from market j to market i. Greenwood-Nimmo et al. (2015a) stress that, due to the order-invariance of GVDs, the variables in $\boldsymbol{y}_t$ can be re-ordered as necessary to support any desired block structure.[4] Using this block structure, we may define the total within-market FEV contribution for market i as follows:

$$\mathcal{W}^{(h)}_{i\leftarrow i} = \frac{1}{m}\mathbf{e}'_m \mathbf{B}^{(h)}_{i\leftarrow i}\mathbf{e}_m \quad (7)$$

where $\mathbf{e}_m$ is an $m \times 1$ vector of ones. As such, $\mathcal{W}^{(h)}_{i\leftarrow i}$ measures the proportion of the h-step-ahead FEV of $\mathbf{y}_{it}$ explained by shocks to $\mathbf{y}_{it}$. $\mathcal{W}^{(h)}_{i\leftarrow i}$, can be decomposed into common-variable FEV contributions within market i, $\mathcal{O}^{(h)}_{i\leftarrow i}$ and cross-variable effects, $\mathcal{C}^{(h)}_{i\leftarrow i}$, as follows:

$$\mathcal{O}^{(h)}_{i\leftarrow i} = \frac{1}{m}\text{trace}\left(\mathbf{B}^{(h)}_{i\leftarrow i}\right) \quad \text{and} \quad \mathcal{C}^{(h)}_{i\leftarrow i} = \mathcal{W}^{(h)}_{i\leftarrow i} - \mathcal{O}^{(h)}_{i\leftarrow i}. \quad (8)$$

[4]To provide a clear and concise exposition, the derivation of the block aggregation routine presented here focuses on connectedness among markets. This is the case that we will consider in Table 2 and Figure 3 below. We will also present results for the connectedness among groups of common moments (i.e. returns for all markets, RNV innovations for all markets and RNS innovations for all markets) in Table 3 and Figure 4 below. It is straightforward to adapt the method presented here to evaluate connectedness among groups of common moments. One first reorders the variables in the VAR to obtain $\mathbf{y}_t = (\mathbf{r}_t, \mathbf{v}_t, \mathbf{s}_t)'$ where $\mathbf{r}_t = (r_{1t}, r_{2t}, \ldots, r_{Nt})$, $\mathbf{v}_t = (v_{1t}, v_{2t}, \ldots, v_{Nt})$ and $\mathbf{s}_t = (s_{1t}, s_{2t}, \ldots, s_{Nt})$ and then aggregates into $g = 3$ groups of common moments, each of which is composed of $m = N$ variables. The block structure used in this case is detailed in the online Technical Supplement.

Note that $\mathcal{O}_{i\leftarrow i}^{(h)}$ measures the proportion of the h-step-ahead FEV of $\mathbf{y}_{it}$ which is not attributable to spillovers among the variables within market i nor to spillovers from other markets to market i. By contrast, $\mathcal{C}_{i\leftarrow i}^{(h)}$ records the total h-step-ahead spillovers between the return, RNV innovation and RNS innovation within market i. The total pairwise directional spillovers from market j to i at horizon h are given by:

$$\mathcal{F}_{i\leftarrow j}^{(h)} = \frac{1}{m}\mathbf{e}_m'\mathbf{B}_{i\leftarrow j}^{(h)}\mathbf{e}_m \tag{9}$$

while the aggregate *from* and *to* connectedness of market i are given by:

$$\mathcal{F}_{i\leftarrow\bullet}^{(h)} = \sum_{j=1,\neq i}^{N} \mathcal{F}_{i\leftarrow j}^{(h)} \quad \text{and} \quad \mathcal{T}_{\bullet\leftarrow i}^{(h)} = \sum_{j=1,\neq i}^{N} \mathcal{F}_{j\leftarrow i}^{(h)} \tag{10}$$

respectively. Finally, the aggregate between-market spillover measure and within-market effect are:

$$\mathcal{S}^{(h)} = \frac{1}{N}\sum_{i=1}^{N} \mathcal{F}_{i\leftarrow\bullet}^{(h)} \quad \text{and} \quad \mathcal{H}^{(h)} = 100 - \mathcal{S}^{(h)}. \tag{11}$$

The interpretation of each of these quantities follows easily from the discussion of the Diebold-Yilmaz method in Section 2.2.

3. Dataset and Risk-Neutral Moments

Our model is estimated using daily returns and the innovations in RNV and RNS for the G10 currencies, with all quotes against the U.S. dollar.[5] We therefore work with the following nine currencies: the Australian dollar (AUD), the British pound (GBP), the Canadian dollar (CAD), the euro (EUR), the Japanese yen (JPY), the New Zealand dollar (NZD), the Norwegian krone (NOK), the Swedish krona (SEK) and the Swiss franc (CHF). Our sample spans the period since the introduction of the euro, from January 1999 to October 2014.

We compute the daily return for the i-th currency as the log-difference of the spot exchange

[5] We also consider a model including innovations in risk-neutral kurtosis (RNK) but find this to yield little empirical benefit, as demonstrated in the online Technical Supplement. RNK is also found to be relatively unimportant in an empirical sense by Rafferty (2012). In general, to the extent that investors are concerned about mass in the tails of the expected distribution of future exchange rate changes, their preferences will tend to be strongly asymmetric and this will be captured by the RNS.

rate, S_{it}, which is measured in units of U.S. dollars per foreign currency unit and is sourced from WM/Reuters via Datastream. We compute the risk-neutral moments following the model-free framework developed by Bakshi and Madan (2000), Carr and Madan (2001) and Bakshi et al. (2003) and applied to foreign exchange options by Jurek (2014). The computation requires appropriate forward exchange rate data, an annualised domestic interest rate and a set of at-the-money and out-of-the-money call and put options. We gather daily one month forward exchange rate data for each currency quoted against the U.S. dollar from WM/Reuters via Datastream. For the interest rate, we use daily data on U.S. eurocurrency interbank money market interest rates with a maturity of one month collected from the Financial Times and ICAP via Datastream. Finally, daily quotes for over-the-counter European FX options with a maturity of 1 month are provided by J.P. Morgan. The options data is quoted in the form of implied volatilities for portfolios of out-of-the-money 25δ and 10δ options contracts as well as an at-the-money delta-neutral (0δ) straddle. From these, we extract the relevant strike prices and options prices using the Garman and Kohlhagen (1983) formulae. Using these, we then compute the model-free risk-neutral moments. Further details of the computation of the risk-neutral moments may be found in the online Technical Supplement.

Following the approach adopted by Menkhoff et al. (2012) and Chang et al. (2013), we work with the innovations in RNV and RNS rather than their levels. The RNV innovations for the i-th market, v_{it}, are extracted as the residuals from the following auxiliary first order autoregression:

$$v_{it} = \mathrm{VOL}_{it}^{RN} - \widehat{\phi}_{iv}\mathrm{VOL}_{i,t-1}^{RN} - \widehat{\mu}_{iv}, \tag{12}$$

where VOL_{it}^{RN} denotes the option-implied risk-neutral volatility for currency i at time t and where Greek letters denote the estimated model parameters. We compute the RNS innovations, s_{it}, in the same manner. The use of innovations confers two benefits. First, it allows us to account for the serial correlation in the risk-neutral moments without including a large number of lags in our VAR model. This allows us to work with shorter rolling samples and, thereby, to achieve richer patterns of time variation. Second, it allows us to focus on unexpected changes in RNV and RNS which reflect unexpected changes in the investment opportunity set facing investors.

4. Full-Sample Analysis

4.1. Connectedness among Variables over the Full Sample

To establish a point of reference, we first study connectedness over the full sample. We estimate a VAR(1) model, where the VAR lag length is selected using the Schwarz criterion. In order to compute the connectedness matrix in (3), one must first choose an appropriate forecast horizon. However, as there is no simple method to select an optimal horizon, we experiment with $h \in \{5, 10, 15\}$, a range which encompasses the values used in most existing applications of the Diebold-Yilmaz framework to daily data. In practice, the connectedness matrix is highly robust to the choice of forecast horizon. The Frobenius norms for $\mathbb{C}^{(5)}$, $\mathbb{C}^{(10)}$ and $\mathbb{C}^{(15)}$ are 277.118, 277.117 and 277.117 respectively, indicating that the three connectedness matrices are almost identical, an observation which is substantiated by elementwise comparison of the matrices (available on request). We therefore adopt $h = 10$ throughout our full-sample analysis without loss of generality. We shall return to the issue of robustness in the context of rolling regression analysis in Section 5.

Table 1 presents the full-sample ten-days-ahead 27×27 variable connectedness matrix. This matrix fully quantifies the magnitude of all pairwise linkages among individual variables in the network. Own-variable effects are contained along the main diagonal, while off-diagonal elements represent directional spillovers. Several features are noteworthy. Firstly, consider spillovers affecting returns. Given the premise that portfolio rebalancing in response to changes in the risk-return profiles of a set of currencies is an important feature of FX markets, one may expect to see strong cross-market spillovers among returns. This is indeed the case over the full sample and is consistent with currency comovements driven by investors rebalancing positions in multiple currencies simultaneously in response to shocks, as documented by Elyasiani and Kocagil (2001), Cai et al. (2008) and Greenwood-Nimmo et al. (2015b).

— Insert Table 1 about here —

Table 1 shows that cross-market spillovers between the returns on different currencies account for more than 50% of the return FEV in most cases. Own-variable effects, by contrast, typically account for only 20–30% of the ten-days-ahead FEV. Spillovers among returns are particularly strong where currencies share an underlying linkage. This is especially true of the European currencies as well as the commodity currencies (AUD, CAD and NZD). Within these groups of currencies, many of the bilateral return spillovers are of the order of 10-15%. Such strong bilateral return spillovers among a subset of currencies suggests a degree of common rebalancing activity affecting these currencies. For example, investors may elect to simultaneously reduce their exposure to the entire set of commodity currencies in the event of an adverse shock to commodity prices.

While cross-market spillovers between returns dominate for most currencies, the JPY emerges as a notable special case. Cross-market return spillovers from other currencies account for a mere 14% of the JPY return FEV. By contrast, the own-variable effect for JPY returns is 52%, which is considerably stronger than in any other currency market. The relative disconnect of JPY returns from the returns of other currencies strongly supports the notion that the JPY is a safe haven currency (Ranaldo and Söderlind, 2010).

In the case of RNV innovations, the distinguished literature on volatility transmission furnishes a strong prior expectation — volatility has been repeatedly shown to spread rapidly and forcefully among FX markets (e.g. Engle et al., 1990; Fleming et al., 1998). This is readily apparent in Table 1. Own-variable effects for RNV innovations account for between 17% (EUR) and 27% (JPY) of the ten-days-ahead FEV, with an average value of 20%. By contrast, spillovers between RNV innovations across currencies are much stronger, ranging from 59% (JPY) to 77% (EUR), a finding which is also consistent with the role of a global FX volatility factor in driving the RNV innovations of individual currencies (Menkhoff et al., 2012). As with return spillovers, strong bilateral volatility spillovers are evident between currencies that share an underlying linkage. For the commodity currencies, common exposure to commodity price volatility provides an appealing explanation for this phenomenon. Meanwhile, among the European currencies, joint exposure to common sources of uncertainty (related to geopolitical linkages, for example) is likely to play an important role. Lastly, the safe haven status of the JPY is again apparent, as the JPY is considerably less susceptible to cross-market RNV spillovers than other currencies.

RNS innovations experience considerably stronger own-variable effects than either returns or RNV innovations and, by construction, commensurately weaker spillovers from the system. There is marked heterogeneity across markets, with the own-variable effects for RNS innovations varying in the range 64% (NZD) to 91% (CAD) and taking an average value of 76%. Currencies' upside and downside crash risks are more strongly influenced by currency-specific idiosyncratic shocks than is the case for either returns or RNV innovations. This is in line with the limited literature on skewness spillovers in equity markets, which emphasises the role of local factors (Hashmi and Tay, 2007, 2012). Nevertheless, more closely related currency pairs exhibit stronger bilateral skewness spillovers — for example the NOK-SEK and AUD-NZD pairs — which suggests that exposure to common shocks may induce a degree of common crash risk.

4.2. Connectedness among Markets and among Moments over the Full Sample

Over the full-sample, it is possible to meaningfully interpret the 729 elements of the 27x27 variable connectedness matrix shown in Table 1. However, this rapidly becomes burdensome when working with subsamples and wholly infeasible in the context of rolling regression analysis. As noted above, block aggregations of the connectedness matrix may be used to focus the analysis as desired and measure spillovers among groups of variables. We briefly consider two cases here, both of which will be used extensively in the rolling-sample analysis below. Table 2 presents the 9×9 market connectedness matrix, which contains total within-market effects for each currency along the prime diagonal and total directional spillovers between currency market pairs in the off-diagonal entries. Adopting the nomenclature proposed by Engle et al. (1990), the within-market effects can be thought of as heatwave effects while the cross-market spillovers are akin to meteor showers. Presenting the market connectedness matrix in this way highlights the key interactions among markets noted above. In the majority of markets, the heatwave effect accounts for less than 50% of the FEV and spillovers from other markets typically exert a dominant influence. Currencies which share an underlying linkage experience stronger bilateral spillovers and the safe haven status of the JPY is easily seen by the strong within-market effect and relatively low cross-market spillovers.

— Insert Table 2 about here —

Similarly, Table 3 reports the 3×3 moment connectedness matrix which measures the full-sample connectedness among returns, RNV and RNS innovations aggregated over all 9 markets. In this case, within-moment effects are recorded along the prime diagonal, with spillovers across moments occupying the off-diagonal positions. This representation of the connectedness matrix focuses attention specifically on interactions between returns and innovations in RNV and RNS. This allows for a clear characterisation of risk spillovers onto returns (as investors rebalance their portfolios in response to changes in risk) and also of return spillovers onto risk meaures (as rebalancing activity and changes in returns feed back into the risk measures).

— Insert Table 3 about here —

Close inspection of Table 3 reveals that spillovers among variables of the same type (e.g. spillovers among returns or spillovers among RNV innovations) are by far the dominant force in the system over the full sample, accounting for more than 80% of FEV in each case. Nonetheless, spillovers between returns, RNV innovations and RNS innovations are non-negligible, implying that there exists a bidirectional relationship where returns adjust in response to innovations in the option-implied moments and vice-versa. However, as stressed by Diebold and Yilmaz (2014), the full sample connectedness measures only characterise *unconditional* linkages over the full sample. In practice, it is likely that the linkages between returns and changes in risk will vary over time, particularly to the extent that currency risk premia are countercyclical (Lustig, Roussanov, and Verdelhan, 2014). Such issues can be analysed using rolling regression to construct *conditional* connectedness measures. It is to this issue that we now turn.

5. Rolling-Sample Analysis

An important choice in the context of rolling regressions is that of the window length. Existing applications of the DY method based on daily data have used a range of values — for example, the main results in Diebold and Yilmaz (2014) are based on $w = 100$ days while Baruník et al. (2015, in press) use $w = 200$ days. Given this uncertainty, the emergent norm in the literature is to evaluate the sensitivity of the rolling connectedness measures to several candidate window lengths. Adopting this approach, we consider candidate values in the set $w \in \{200, 250, 300\}$ trading days. Furthermore, we consider candidate forecast horizons in the set $h \in \{5, 10, 15\}$ trading days to verify that the robustness of our full-sample results to the choice of forecast horizon also extends to rolling-sample analysis. Lastly, for completeness, we investigate the effect of adopting Diebold and Yilmaz's (2009) earlier approach to measuring connectedness which employs orthogonalised forecast error variance decompositions (OVDs) rather than GVDs. Consequently, the design of our sensitivity analysis closely follows that of Diebold and Yilmaz (2014, section 5.3.4).[6]

— Insert Figure 1 about here —

Figure 1 reveals that neither the choice of forecast horizon nor of window length exerts a major influence on our results. The time series behaviour of the aggregate spillover index defined in (5) is remarkably similar in all cases. Furthermore, the correlation between the spillover indices based on GVDs and the mean of the spillover indices based on OVDs under 1,000 random variable orderings is no lower than 0.95 in any case, although there is a slight level shift separating the two sets of results. Diebold and Yilmaz (2014, p. 130) observe the same effect and note that the aggregate spillover activity computed using OVDs acts as a lower bound on that derived from GVDs. Overall, the GVD results may be considered more accurate because they accommodate the full correlation structure of the reduced form VAR disturbances.

5.1. Aggregate Spillover Activity over Time

In light of Figure 1, the remainder of our analysis focuses on the GVD case with $w = 250$ trading days and $h = 10$ trading days without loss of generality. This case corresponds to the central panel of Figure 1. Figure 2 shows the aggregate spillover index in this case, enlarged and annotated with the timing of several major events. The figure reveals substantial time variation. Spillovers begin to rise in late 2000 following the collapse of the dotcom bubble and the ensuing U.S. recession. They continue to rise during the Federal Reserve's monetary accommodation from 2001–4. Spillover activity then gradually recedes with the normalisation of U.S. interest rates until the onset of the subprime mortgage crisis in 2007, with a particularly rapid intensification of spillover activity following the collapse of Lehman Brothers in September 2008. Spillovers remain at a high level during the GFC and for several years thereafter during the European sovereign debt crisis before receding in late 2012 with the gradual abatement of the debt crisis.

[6] Unlike many existing applications of the DY approach which simply impose the same VAR lag length in every rolling sample, we select the lag length for the r-th rolling regression from the set $p_r \in \{1, 2, \ldots, 5\}$ using the Schwarz criterion. In practice, VAR(1) is selected in every rolling sample.

— Insert Figure 2 about here —

5.2. Connectedness among Markets over Time

Figure 3 summarises the time-varying connectedness among markets. Working at this level of aggregation allows us to identify which currency markets are more (or less) integrated and how this changes over time. The figure is composed of nine panels, one for each market. The panel for the ith market contains an upper plot showing the within-market heatwave effect, $\mathcal{W}_{i\leftarrow i}^{(10)}$ and a lower plot showing the total inward and outward spillovers for market i, $\mathcal{F}_{i\leftarrow\bullet}^{(10)}$ and $\mathcal{T}_{\bullet\leftarrow i}^{(10)}$, respectively.

— Insert Figure 3 about here —

Consider the top row, which contains the commodity currencies, AUD, NZD and CAD. In each case, the within-market effect is very high at the start of the sample (approximately 70% of market FEV), indicating strong idiosyncratic variation and relatively weak integration with the other markets in the system. However, this changes markedly over the sample period, dropping to around 30% during the GFC. Between-market spillover activity — both inward and outward — increases markedly at this time, reflecting much greater integration of the commodity currencies with the system as a whole. Greater integration of commodity currencies is likely to reflect the marked financialisation of commodity markets during our sample period (Cheng and Xiong, 2014).

The European currencies (EUR, NOK, SEK) appear on the middle row. Along with the CHF, this group displays markedly common behaviour, with low within-market (idiosyncratic) effects throughout the sample matched by strong between-market spillovers. This indicates that the European currencies are closely integrated, while the positive net spillovers (outward spillovers exceed inward spillovers) arising from the EUR and the CHF over much of the sample suggest that these are the leading markets within the group, as one would expect. Finally, the JPY and, to a lesser extent, the GBP exhibit somewhat more idiosyncratic variation than the other currencies which is matched by weak between-market spillovers. These two currencies are relatively weakly integrated with the other markets, indicating that they may offer a safe haven to FX investors. This is true of the GBP early in the sample and of the JPY throughout the sample.

5.3. Connectedness among Moments over Time

Figure 4 records the evolution of connectedness among moments over rolling samples. The figure contains nine panels, each of which contains two plots. The upper plot shows the connectedness among moments within the same market and the lower plot shows the connectedness among moments between markets.[7] Consequently, Figure 4 enables us to investigate the relative importance over time of idiosyncratic currency-specific effects and of systematic cross-market spillovers affecting returns, RNV innovations and RNS innovations, respectively. It also allows us to investigate changes in the interaction between returns and innovations in RNV and RNS over time. As mentioned above, the countercyclical currency risk premia described by Lustig et al. (2014) are likely to result in stronger interactions between returns and innovations in RNV and RNS in bad times over the business cycle as returns become more sensitive to changes in risk and vice versa.

— Insert Figure 4 about here —

Focus initially on the upper row of the figure, which reports the evolution of the spillovers affecting returns over our sample period. As with the full-sample results documented above, the own-variable within-market effect in returns is relatively weak, always remaining below 40% and declining substantially during the GFC. Spillovers among returns between markets are much stronger in general, peaking at 68% in 2005 before dipping during the GFC. Meanwhile, spillovers to returns from RNV and RNS innovations increase substantially during the GFC and the European sovereign debt crisis, reaching a combined high of nearly 50% in October 2008 shortly after the collapse of Lehman Brothers. This is a clear indication of a marked increase in investors' sensitivity to risk during the crises. Furthermore, given that the large majority of spillovers to returns from RNV and RNS innovations occurs between markets, one may infer that investors were particularly concerned with systematic risk (aggregate FX uncertainty and crash risk in particular).

The second row of Figure 4 focuses on spillovers affecting RNV innovations. As with returns, the own-variable within-market effect in RNV innovations is relatively weak and has gradually fallen

[7]The structure of Figure 4 maps onto the structure of Table 3 except that each element of the table is decomposed into a within-market and a between-market effect using a similar method to that described in (8). Full computational details are provided in the online Technical Supplement.

across our sample. By contrast, between-market spillovers among RNV innovations have gradually intensified from roughly 50% at the start of our sample to more than 65% towards the end of the sample, indicating that systematic volatility linkages dominate the effect of idiosyncratic volatility. In addition, cross-market spillovers from returns to RNV innovations strengthen considerably in the aftermath of the GFC and during the European sovereign debt crisis. Consequently, our results indicate that investors' expectations of future exchange rate volatility are heavily conditioned on realised exchange rate movements and vice versa, at least in times of stress. This is a clear manifestation of the feedback effects between rebalancing activity and risk measures outlined in our opening remarks and it underscores the value of network models in this context.

The last row of Figure 4 reveals that the own-variable within-market effect in RNS innovations (i.e. the idiosyncratic variation in skewness) is much stronger than is the case with either returns or RNV innovations. Furthermore, it displays marked time variation, falling dramatically during the GFC and European debt crisis from 50% of FEV to less than 25%. This is mirrored by an increase in between-market spillovers among RNS innovations. The intensification of skewness spillovers across markets during turbulent times suggests that coordinated crash risk is more prevalent during times of financial stress, as the likelihood of carry trade positions having to be unwound due to liquidity constraints increases (Brunnermeier et al., 2009; Rafferty, 2012). Finally, we also observe a large increase in spillovers from returns to RNS innovations during the GFC and the European sovereign debt crisis, which indicates that investors' forward-looking perceptions of crash risk are heavily conditioned on realised exchange rate movements, as one may expect.

6. Relationship to Macroeconomic and Financial Conditions

Careful consideration of our rolling-sample results suggests two interesting phenomena which may be discerned most easily in relation to the aggregate spillover index in Figure 2. First, it appears that FX spillovers evolve countercyclically. Second, FX spillovers intensify in times of financial stress, most notably during the GFC and the European sovereign debt crisis. Both effects are demonstrated in Figure 5, which plots the rolling spillover index shown in Figure 2 alongside the 250-day rolling average of the federal funds rate, the TED spread and the VIX, respectively. The use of rolling averages provides a measure of the low frequency movements of each series which lends itself to a medium- or long-term interpretation.

— Insert Figure 5 about here —

The federal funds rate is a gauge of the cyclical position of the U.S. economy. Figure 5 shows a remarkably strong negative relationship between aggregate FX spillovers and the federal funds rate, indicating a clear countercyclical pattern. The correlation is -0.54 over the full sample and -0.71 in the period up to December 2008 when active interest rate policy was curtailed by the zero lower bound (ZLB). This striking correlation is consistent with a U.S. dollar factor driving exchange rate dynamics and linkages in FX markets (Lustig, Roussanov, and Verdelhan, 2011) and is highly suggestive of countercyclical currency risk premia relative to the U.S. dollar (Lustig et al., 2014). One can envisage a number of mechanisms underlying the countercyclicality of aggregate spillover activity. For example, risk-averse investors may become more responsive to changes in the risk environment during downturns, leading to an intensification of spillovers from risk measures to returns. Such a change is also likely to be reflected in the options data due to hedging activity, thereby strengthening spillovers from realised returns to RNV and RNS innovations.

The TED spread is a common proxy for credit risk and funding liquidity in the interbank money market. It is the spread between the three-month U.S. LIBOR rate and the three-month U.S. Treasury Bill rate. Mancini, Ranaldo, and Wrampelmeyer (2013) show that when the TED spread increases, market-wide FX liquidity decreases. When the TED spread spikes — as it did in the GFC, especially after the collapse of Lehman Brothers — funding liquidity dries up, forcing investors to rapidly unwind their long positions. As described by Rafferty (2012), this is likely to induce coordinated crashes in the FX markets. Consequently, the relationship between FX spillover activity and the TED spread is likely to be positive, and strongly so during the GFC. This is exactly what we see in the central panel of Figure 5. Over the full sample, we observe a modest positive correlation of 0.11 which rises to 0.42 when evaluated over the period since September 2008.

Lastly, the bottom panel of Figure 5 relates to the VIX, which is an option-implied measure of expected volatility for the S&P500 and which has been widely adopted as a proxy for investors' fear and uncertainty. The figure reveals an unambiguous positive correlation between FX spillovers and the VIX. The correlation stands at a moderate 0.33 over the full sample but rises to 0.75 in the period since September 2008. One would expect such a strongly positive correlation if risk-averse investors elect to rebalance their portfolios and adjust their hedging strategies more often and/or more substantially in an uncertain environment. This is consistent with the idea that many investors reduce their exposure to risky assets in periods of elevated uncertainty.

To complement the preceding low frequency analysis, we examine the extent to which large changes in the spillover index occur in conjunction with large changes to the federal funds rate, the TED spread or the VIX. To this end, we construct the following binary indicators to identify periods in which the rolling spillover index, $S_t^{(h)}$, reaches a new 250-day high or low, respectively:

$$\overline{S_t}^{(h)} = \mathbb{1}\left\{S_t^{(h)} - \max\left(S_{t-1}^{(h)}, \ldots, S_{t-250}^{(h)}\right) > 0\right\} \;\; \& \;\; \underline{S_t}^{(h)} = \mathbb{1}\left\{S_t^{(h)} - \min\left(S_{t-1}^{(h)}, \ldots, S_{t-250}^{(h)}\right) < 0\right\}$$

where $\mathbb{1}\{\cdot\}$ is an indicator function which takes the value one if the condition in braces is satisfied and zero otherwise. We apply the same procedure to define 250-day high and low indicator variables for the federal funds rate ($\overline{F_t}$ and $\underline{F_t}$), the TED spread ($\overline{T_t}$ and $\underline{T_t}$) and the VIX ($\overline{V_t}$ and $\underline{V_t}$). We then use these indicators to compute an array of pseudo-hit-rates. For example, the pseudo-hit-rate capturing occasions on which the spillover index records a new 250-day high *and* the federal funds rate records a new 250-day low within ± 5 days is given by:

$$\mathbb{H}\left(\overline{S_t}^{(h)}, \underline{F_t}\right) = \left(\frac{\sum_{t=w+1}^{T} \mathbb{1}\left\{\left(\overline{S_t}^{(h)} \times \sum_{i=-5}^{5} \underline{F_{t+i}}\right) \neq 0\right\}}{\sum_{t=w+1}^{T} \overline{S_t}^{(h)}}\right) \times 100\% \tag{13}$$

In light of Figure 5, given that the spillover index is negatively correlated with the federal funds rate and positively correlated with the TED spread and the VIX, we compute the following pseudo-hit-rates: $\mathbb{H}\left(\overline{S_t}^{(h)}, \underline{F_t}\right)$, $\mathbb{H}\left(\underline{S_t}^{(h)}, \overline{F_t}\right)$, $\mathbb{H}\left(\overline{S_t}^{(h)}, \overline{T_t}\right)$, $\mathbb{H}\left(\underline{S_t}^{(h)}, \underline{T_t}\right)$, $\mathbb{H}\left(\overline{S_t}^{(h)}, \overline{V_t}\right)$ and $\mathbb{H}\left(\underline{S_t}^{(h)}, \underline{V_t}\right)$. The results are reported in Table 4, while Figure 6 records the timing of the respective hits.

— Insert Table 4 and Figure 6 about here —

The hit-rate with respect to the federal funds rate is relatively high over the full sample despite the ZLB constraint which has seen relative constancy of the effective funds rate since December 2008. When considered only over the pre-ZLB period, the hit rate is quite remarkable, with 62% of spillover highs occurring within ± 5 days of a funds rate low and 35% of spillover lows within ±5 days of a funds rate high. Hence, FX market participants appear to respond rapidly to signals arising from U.S. monetary policy, particularly where the signal is of a deterioration in U.S. macroeconomic and financial conditions. This aligns with the findings of Fischer and Ranaldo (2011), who demonstrate that global FX trading volume increases after meetings of the Federal Open Market Committee, which is suggestive of increased portfolio rebalancing activity. Consulting Figure 6, it is clear that hits with respect to the federal funds rate occur throughout the pre-ZLB period. Spillover highs are associated with funds rate lows during both the Federal Reserve's prolonged monetary accommodation between 2001 and 2003 (related to the U.S. recession following the collapse of the dotcom bubble) and the subsequent monetary easing associated with the GFC. Furthermore, many spillover lows coincide with funds rate highs in the period of increasing U.S. interest rates prior to the onset of the subprime mortgage crisis in 2007.

Hit-rates with respect to the TED spread and the VIX are relatively low over the full sample but are much higher in the period of financial turbulence since the collapse of Lehman Brothers. This is particularly true of the VIX, where almost half of all spillover highs in this period occur within ±5 days of a corresponding VIX high and a third of spillover lows correspond to a VIX low, a finding which confirms that FX trading activity is strongly associated with investor sentiment. Furthermore, Figure 6 reveals that large swings in spillover activity may be driven in large part by funding liquidity effects, as hits with respect to the TED spread occur only during periods where the spillover index is either rising or falling particularly dramatically.

7. Conclusion

We study the interaction between FX returns and the innovations in the option-implied RNV and RNS for the G10 currencies. Our use of risk-neutral moments accords with recent developments in the literature, which stress their benefits over realised risk measures in terms of their forward-looking nature and their model-free computation (Bakshi and Madan, 2000; Carr and Madan, 2001; Bakshi et al., 2003). Our analysis employs an empirical network model derived from a generalisation of the connectedness methodology of Diebold and Yilmaz (2009, 2014).

Several interesting results emerge from our analysis. Firstly, over the full sample period, we observe strong spillovers among returns, with particularly notable bilateral spillovers among currencies which share an underlying linkage, such as those which are exposed to common shocks. Similarly, spillovers among RNV innovations across currencies account for as much as 75% of the ten-days-ahead FEV of RNV innovations, indicating that systematic volatility plays a dominant role while idiosyncratic volatility is much less important on average. However, over the full sample, the opposite is true of RNS innovations, where idiosyncratic factors play an important role in driving the measured risk of large jumps and crashes in exchange rates.

Rolling-sample analysis reveals significant time variation in both the pattern and intensity of spillovers. A general tendency towards increased spillovers among markets during the GFC and the sovereign debt crisis is apparent. Importantly, we see a large increase in interactions among returns and innovations in risk measures as investors become more responsive to risk during times of financial stress. We also observe increased cross-market connectedness among innovations in RNV and RNS, which implies greater common behaviour of forward-looking measures of risk. Spillovers of RNS innovations between markets intensify particularly markedly at this time, highlighting the role of coordinated crash risk during the crises. Finally, we demonstrate that spillover activity among FX markets evolves countercyclically, rising during periods of financial stress and also rising when domestic conditions in the U.S. deteriorate. One can readily envisage mechanisms which may account for these changing patterns of spillover behaviour, at least in part. The development of models to formalise such mechanisms represents a fruitful avenue for continuing research.

References

Ang, A., Hodrick, R. J., Xing, Y., Zhang, X., 2006. The Cross-Section of Volatility and Expected Returns. Journal of Finance 61, 259–299.

Ang, A., Hodrick, R. J., Xing, Y., Zhang, X., 2009. High Idiosyncratic Volatility and Low Returns: International and Further US Evidence. Journal of Financial Economics 91, 1–23.

Bakshi, G., Kapadia, N., Madan, D., 2003. Stock Return Characteristics, Skew Laws and the Differential Pricing of Individual Equity Options. Review of Financial Studies 16, 101–143.

Bakshi, G., Madan, D., 2000. Spanning and Derivative-Security Valuation. Journal of Financial Economics 55, 205–238.

Bakshi, G., Panayotov, G., 2013. Predictability of Currency Carry Trades and Asset Pricing Implications. Journal of Financial Economics 110 (1), 139–163.

Baruník, J., Kočenda, E., Vácha, L., 2015, in press. Asymmetric Connectedness on the U.S. Stock Market: Bad and Good Volatility Spillovers. Journal of Financial Markets.

Billio, M., Getmansky, M., Lo, A., Pelizzon, L., 2012. Econometric Measures of Connectedness and Systemic Risk in the Finance and Insurance Sectors. Journal of Financial Economics 104, 535–559.

Brunnermeier, M. K., Nagel, S., Pedersen, L. H., 2009. Carry Trades and Currency Crashes. NBER Macroeconomics Annual 2008 23, 313–347.

Bubák, V., Kočenda, E., Žikeš, F., 2011. Volatility Transmission in Emerging European Foreign Exchange Markets. Journal of Banking and Finance 35, 2829–2841.

Burnside, C., Eichenbaum, M., Kleshchelski, I., Rebelo, S., 2011. Do Peso Problems Explain the Returns to the Carry Trade? Review of Financial Studies 24, 853–891.

Cai, F., Howorka, E., Wongswan, J., 2008. Informational Linkage Across Trading Regions: Evidence from Foreign Exchange Markets. Journal of International Money and Finance 27, 1212–1243.

Carr, P., Madan, D., 2001. Optimal Positioning in Derivative Securities. Quantitative Finance 1, 19–37.

Chang, B. Y., Christoffersen, P., Jacobs, K., 2013. Market Skewness Risk and the Cross-Section of Stock Returns. Journal of Financial Economics 107, 46–68.

Chen, Y.-C., Gwati, R., 2014. Understanding Exchange Rate Dynamics: What does the Term Structure of FX Options Tell Us? Mimeo, Washington University.

Cheng, I.-H., Xiong, W., 2014. Financialization of Commodity Markets. Annual Review of Financial Economics 6, 419–441.

Christoffersen, P., Jacobs, K., Chang, B. Y., 2013. Forecasting with Option-Implied Information. In: Elliott, G., Timmermann, A. (Eds.), Handbook of Economic Forecasting. Vol. 2A. North-Holland, Amsterdam, pp. 581–656.

Conrad, J., Dittmar, R. F., Ghysels, E., 2013. Ex Ante Skewness and Expected Stock Returns. The Journal of Finance 68, 85–124.

Diebold, F., Yilmaz, K., 2009. Measuring Financial Asset Return and Volatility Spillovers, with Application to Global Equity Markets. Economic Journal 119, 158–171.

Diebold, F., Yilmaz, K., 2014. On the Network Topology of Variance Decompositions: Measuring the Connectedness of Financial Firms. Journal of Econometrics 182, 119–134.

Elyasiani, E., Kocagil, A., 2001. Interdependence and Dynamics in Currency Futures: A Multivariate Cointegration Analysis of Intra-day Data. Journal of Banking and Finance 25, 1161–1186.

Engle, R. F., Ito, T., Lin, W.-L., 1990. Meteor Showers or Heat Waves? Heteroskedastic Intra-daily Volatility in the Foreign Exchange Market. Econometrica 58, 525–524.

Fischer, A. M., Ranaldo, A., 2011. Does FOMC News Increase Global FX Trading? Journal of Banking and Finance 35, 2965–2973.

Fleming, J., Kirby, C., Ostdiek, B., 1998. Information and Volatility Linkages in the Stock, Bond, and Money Markets. Journal of Financial Economics 49, 111–137.

Garman, M. B., Kohlhagen, S. W., 1983. Foreign Currency Option Values. Journal of International Money and Finance 2, 231–237.

Greenwood-Nimmo, M. J., Nguyen, V. H., Shin, Y., 2015a. Measuring the Connectedness of the Global Economy.

Mimeo, University of Melbourne.

Greenwood-Nimmo, M. J., Nguyen, V. H., Shin, Y., 2015b. Quantifying Informational Linkages in a Global Model of Currency Spot Markets. Working Paper No. 2443243, SSRN.

Hashmi, A. R., Tay, A. S., 2007. Global Regional Sources of Risk in Equity Markets: Evidence from Factor Models with Time-Varying Conditional Skewness. Journal of International Money and Finance 26, 430–453.

Hashmi, A. R., Tay, A. S., 2012. Mean, Volatility and Skewness Spillovers in Equity Markets. In: Bauwens, L., Hafner, C., Laurent, S. (Eds.), Handbook of Volatility Models and Their Applications, 1st Edition. John Wiley and Sons, Ch. 5, pp. 127–145.

Hong, Y., 2001. A Test for Volatility Spillover with Application to Exchange Rates. Journal of Econometrics 103 (1), 183–224.

Jurek, J. W., 2014. Crash-Neutral Currency Carry Trades. Journal of Financial Economics 113, 325–347.

Kearney, C., Patton, A. J., 2000. Multivariate GARCH Modeling of Exchange Rate Volatility Transmission in the European Monetary System. Financial Review 35 (1), 29–48.

Lustig, H., Roussanov, N., Verdelhan, A., 2011. Common Risk Factors in Currency Markets. Review of Financial Studies 24, 3731–3777.

Lustig, H., Roussanov, N., Verdelhan, A., 2014. Countercyclical Currency Risk Premia. Journal of Financial Economics 111, 527–553.

Mancini, L., Ranaldo, A., Wrampelmeyer, J., 2013. Liquidity in the Foreign Exchange Market: Measurement, Commonality, and Risk Premiums. The Journal of Finance 68, 1805–1841.

Melvin, M., Melvin, B. P., 2003. The Global Transmission of Volatility in the Foreign Exchange Market. Review of Economics and Statistics 85 (3), 670–679.

Menkhoff, L., Sarno, L., Schmeling, M., Schrimpf, A., 2012. Carry Trades and Global Foreign Exchange Volatility. The Journal of Finance 67, 681–718.

Nikkinen, J., Sahlström, P., Vähämaa, S., 2006. Implied Volatility Linkages among Major European Currencies. Journal of International Financial Markets, Institutions and Money 16 (2), 87–103.

Pesaran, M., Shin, Y., 1998. Generalized Impulse Response Analysis in Linear Multivariate Models. Economics Letters 58, 17–29.

Rafferty, B., 2012. Currency Returns, Skewness and Crash Risk. Working Paper 2022920, SSRN.

Ranaldo, A., Söderlind, P., 2010. Safe Haven Currencies. Review of Finance 14, 385–407.

		AUD			CAD			EUR			JPY			NZD			NOK			SEK			CHF			GBP		
		r	v	s	r	v	s	r	v	s	r	v	s	r	v	s	r	v	s	r	v	s	r	v	s	r	v	s
AUD	r	20.4	5.9	1.2	7.8	2.8	0.2	6.2	1.7	0.2	0.0	2.0	0.0	14.1	5.0	1.5	7.2	1.6	0.2	7.4	1.6	0.1	3.3	1.3	0.0	5.9	2.3	0.1
	v	5.4	18.7	0.1	2.0	7.5	0.0	0.8	7.3	0.0	0.8	6.2	0.1	3.5	15.5	0.3	1.5	7.0	0.0	1.2	6.7	0.0	0.1	6.4	0.0	1.3	7.3	0.1
	s	4.6	0.6	69.9	1.9	0.5	0.4	1.8	0.1	0.4	0.0	0.2	0.0	3.5	0.6	5.5	2.1	0.1	1.5	2.0	0.1	1.0	0.9	0.1	0.5	1.3	0.2	0.2
CAD	r	11.3	3.1	0.8	29.8	3.6	0.6	6.0	1.1	0.2	0.0	1.0	0.0	9.0	2.7	0.9	7.8	1.2	0.1	7.9	1.1	0.1	3.2	0.8	0.0	5.8	1.7	0.0
	v	3.2	9.5	0.1	2.9	23.9	0.1	0.4	8.4	0.0	0.8	5.0	0.1	2.2	8.2	0.3	1.4	8.0	0.0	1.1	7.9	0.0	0.0	7.7	0.0	1.0	7.5	0.1
	s	0.7	0.0	0.6	1.6	0.4	91.3	0.7	0.1	0.3	0.2	0.1	0.1	0.6	0.0	0.1	0.5	0.1	0.1	0.5	0.1	0.1	0.6	0.1	0.1	0.5	0.1	0.3
EUR	r	6.5	0.9	0.4	4.3	0.4	0.2	21.2	0.4	1.2	1.3	0.0	0.1	6.2	0.8	0.6	14.0	0.4	0.4	14.7	0.3	0.3	15.1	0.2	0.2	9.4	0.5	0.1
	v	1.4	6.4	0.0	0.6	5.7	0.0	0.3	16.5	0.1	0.8	4.6	0.1	1.0	5.6	0.0	0.6	15.7	0.0	0.5	15.5	0.0	0.0	14.4	0.0	0.4	9.3	0.2
	s	0.8	0.1	0.2	0.5	0.2	0.2	4.4	0.3	72.6	0.5	0.5	0.1	0.8	0.0	0.4	2.7	0.3	1.1	2.7	0.3	1.3	3.5	0.5	1.8	1.8	0.1	2.0
JPY	r	0.0	2.2	0.0	0.0	1.8	0.1	3.1	2.4	0.3	52.4	10.9	4.4	0.1	2.0	0.0	1.4	2.4	0.0	1.2	2.4	0.0	7.1	2.4	0.1	1.0	2.1	0.3
	v	2.6	8.9	0.1	1.0	5.6	0.0	0.0	7.6	0.2	5.6	27.1	0.6	1.8	7.7	0.1	0.2	7.5	0.0	0.2	7.2	0.0	0.4	7.0	0.1	0.4	7.7	0.2
	s	0.0	0.3	0.0	0.0	0.4	0.1	0.4	0.6	0.1	7.5	1.8	82.1	0.0	0.4	0.3	0.1	0.6	0.0	0.1	0.6	1.2	0.9	0.7	0.9	0.1	0.4	0.1
NZD	r	15.8	4.3	0.9	6.9	2.2	0.1	6.7	1.4	0.3	0.0	1.5	0.0	22.9	4.3	1.7	7.4	1.4	0.2	7.4	1.3	0.1	3.7	1.1	0.0	6.5	1.9	0.1
	v	4.9	16.7	0.1	2.0	6.9	0.0	0.8	6.8	0.0	0.8	5.8	0.1	3.9	20.1	0.4	1.6	6.7	0.0	1.2	6.3	0.0	0.1	6.0	0.0	1.4	7.5	0.1
	s	5.2	1.2	5.3	2.3	0.8	0.1	2.3	0.2	0.1	0.0	0.3	0.2	5.3	1.5	63.9	2.7	0.2	0.6	2.9	0.2	1.4	1.1	0.2	0.0	1.5	0.2	0.2
NOK	r	7.6	1.7	0.6	5.6	1.2	0.1	14.1	0.7	0.7	0.6	0.2	0.0	6.9	1.7	0.8	21.4	0.7	0.3	14.8	0.7	0.3	9.5	0.6	0.1	8.1	1.0	0.1
	v	1.4	6.3	0.0	0.7	5.6	0.0	0.3	16.0	0.1	0.8	4.6	0.1	1.0	5.5	0.0	0.6	16.8	0.0	0.5	15.9	0.0	0.0	13.9	0.0	0.5	9.2	0.2
	s	0.5	0.1	1.4	0.3	0.1	0.1	1.6	0.1	1.1	0.0	0.0	0.0	0.5	0.1	0.6	1.1	0.1	68.0	1.2	0.1	17.5	0.9	0.0	3.8	0.7	0.0	0.1
SEK	r	7.8	1.4	0.5	5.7	1.0	0.1	15.0	0.6	0.8	0.5	0.2	0.0	6.9	1.2	0.8	14.9	0.6	0.4	21.6	0.6	0.3	9.6	0.4	0.1	8.1	0.8	0.1
	v	1.3	6.1	0.0	0.6	5.6	0.0	0.3	16.1	0.1	0.8	4.6	0.1	0.9	5.3	0.0	0.5	16.2	0.0	0.5	17.2	0.0	0.0	14.0	0.0	0.4	9.1	0.2
	s	0.4	0.1	1.0	0.2	0.0	0.1	1.4	0.0	1.3	0.0	0.1	0.8	0.5	0.0	1.2	0.9	0.0	16.9	1.1	0.0	68.4	0.9	0.1	3.8	0.7	0.0	0.1
CHF	r	4.4	0.1	0.3	2.9	0.0	0.2	19.6	0.0	1.2	3.8	0.4	0.3	4.5	0.1	0.4	12.2	0.0	0.3	12.4	0.0	0.3	27.6	0.2	0.2	8.4	0.0	0.2
	v	1.2	6.2	0.0	0.5	5.7	0.0	0.2	15.7	0.1	0.9	4.7	0.2	0.9	5.4	0.0	0.5	15.0	0.0	0.3	14.8	0.0	0.2	18.1	0.1	0.3	8.7	0.3
	s	0.2	0.0	0.7	0.1	0.0	0.1	0.8	0.2	2.0	0.1	0.2	0.5	0.2	0.0	0.0	0.5	0.1	4.4	0.5	0.1	4.5	1.0	0.4	82.8	0.3	0.1	0.2
GBP	r	7.7	1.8	0.5	5.2	1.1	0.2	11.8	0.7	0.6	0.5	0.4	0.0	7.5	1.8	0.6	10.1	0.7	0.2	10.0	0.7	0.2	8.1	0.5	0.1	26.5	2.4	0.2
	v	2.3	7.8	0.0	1.2	6.3	0.0	0.5	11.3	0.0	0.8	5.6	0.1	1.6	7.4	0.0	0.9	11.0	0.0	0.8	10.6	0.0	0.0	9.6	0.0	1.9	19.9	0.3
	s	0.2	0.3	0.3	0.1	0.3	0.4	0.7	1.1	2.1	0.4	0.7	0.1	0.3	0.3	0.2	0.6	1.0	0.1	0.5	1.0	0.1	0.8	1.2	0.2	0.8	1.3	84.7

NOTES: The connectedness matrix is computed following Diebold and Yilmaz (2014) using a forecast horizon of $h = 10$ trading days. All values are measured in percentage units and each row sums to 100%. The depth of shading reflects the strength of the associated own-variable/spillover effect, with darker shading indicating a stronger effect.

Table 1: Full-Sample Connectedness among Variables

	AUD	CAD	EUR	JPY	NZD	NOK	SEK	CHF	GBP
AUD	42.27	7.68	6.18	3.12	16.52	7.11	6.69	4.22	6.22
CAD	9.79	51.42	5.73	2.47	8.03	6.40	6.27	4.18	5.70
EUR	5.59	4.04	39.02	2.68	5.16	11.73	11.92	11.90	7.97
JPY	4.73	3.05	4.92	64.12	4.15	4.08	4.30	6.54	4.10
NZD	18.17	7.13	6.21	2.94	41.30	6.91	6.91	4.05	6.39
NOK	6.51	4.55	11.55	2.13	5.70	36.33	16.98	9.62	6.64
SEK	6.20	4.46	11.83	2.35	5.65	16.84	36.51	9.65	6.51
CHF	4.37	3.19	13.30	3.64	3.83	11.00	11.00	43.51	6.16
GBP	6.98	4.93	9.63	2.91	6.53	8.19	7.96	6.84	46.01

NOTE: The market connectedness matrix is computed following Diebold and Yilmaz (2014) under the block aggregation routine devised by Greenwood-Nimmo et al. (2015a) using a forecast horizon of $h = 10$ trading days. All values are measured in percentage units and each row sums to 100%. The depth of shading reflects the strength of the associated within-market/spillover effect, with darker shading indicating a stronger effect.

Table 2: Full-Sample Market Connectedness Matrix among Currency Markets

	r	v	s
r	83.47	13.16	3.37
v	10.00	89.29	0.71
s	10.63	2.90	86.47

NOTE: The moment connectedness matrix is computed following Diebold and Yilmaz (2014) under the block aggregation routine devised by Greenwood-Nimmo et al. (2015a) using a forecast horizon of $h = 10$ trading days. All values are measured in percentage units and each row sums to 100%. The depth of shading reflects the strength of the associated own-moment/spillover effect, with darker shading indicating a stronger effect.

Table 3: Full-Sample Moment Connectedness Matrix

		$\overline{F_t}$	$\underline{F_t}$	$\overline{T_t}$	$\underline{T_t}$	$\overline{V_t}$	$\underline{V_t}$
Full Sample	$\overline{S_t}^{(h)}$		32%	6%		13%	
	$\underline{S_t}^{(h)}$	26%			4%		21%
Pre-ZLB Period	$\overline{S_t}^{(h)}$		62%				
	$\underline{S_t}^{(h)}$	35%					
Crisis Period	$\overline{S_t}^{(h)}$			21%		45%	
	$\underline{S_t}^{(h)}$				6%		33%

NOTE: Following the definition in Section 6, $\overline{x_t}$ ($\underline{x_t}$) is a binary variable indicating periods in which the variable $x_t \in \left\{S_t^{(h)}, F_t, T_t, V_t\right\}$ records a new high (low) relative to its historical values over the preceding 250 trading days. The table reports pseudo-hit-rates computed as in Equation (13). A 'hit' is defined as a new high/low in the spillover index occuring within ±5 trading days of a new high/low in the named macro-financial variable (F_t, T_t or V_t). The full sample is 08-Dec-2000 to 14-Oct-2014 (4,571 trading days), the pre-ZLB sample is 08-Dec-2000 to 31-Dec-2008 (2,077 trading days) and the crisis sample is 15-Sep-2008 to 14-Oct-2014 (1,571 trading days).The aggregate spillover index, $S_t^{(h)}$, is obtained using a rolling window length of $w = 250$ trading days with the forecast horizon set to $h = 10$ trading days.

Table 4: Pseudo-Hit-Rates over the Full Sample and Selected Subsamples

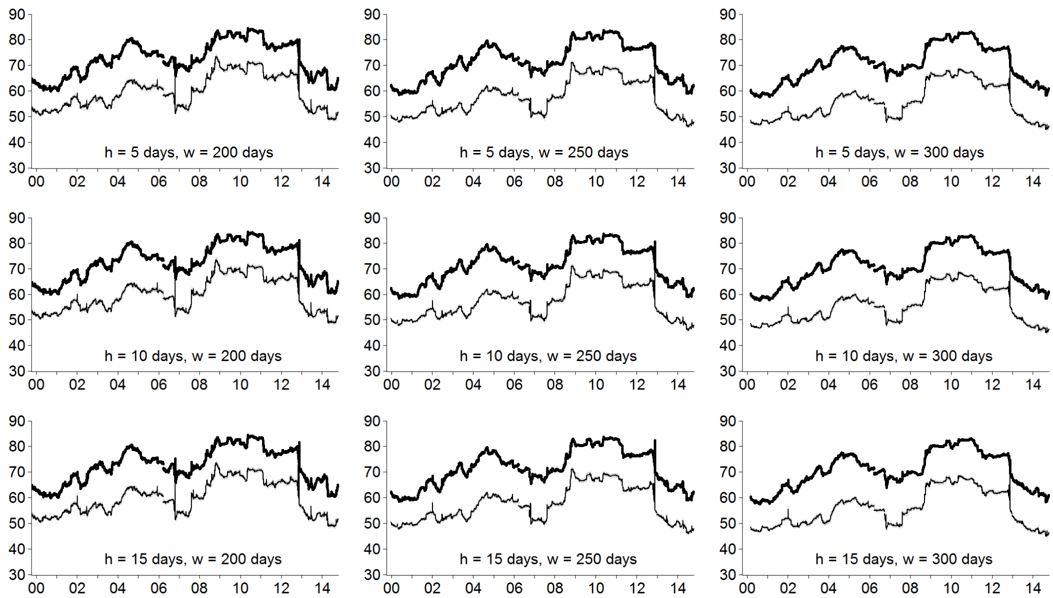

NOTE: We consider windows of $w = (200, 250, 300)$ trading days, predictive horizons of $h = (5, 10, 15)$ trading days and a variety of randomly drawn Cholesky orderings. In each panel, the heavy solid line shows the result using order-invariant GVD, the gray band is the $[10\%, 90\%]$ interval based on 1,000 randomly-selected Cholesky orderings and the fine solid line is the mean under the 1,000 Cholesky orderings. In each case, the correlation between the GVD-based spillover index and the mean of the Cholesky spillover indices is between 0.95 and 0.96.

Figure 1: Sensitivity to Window Length, Forecast Horizon and Orthogonalisation

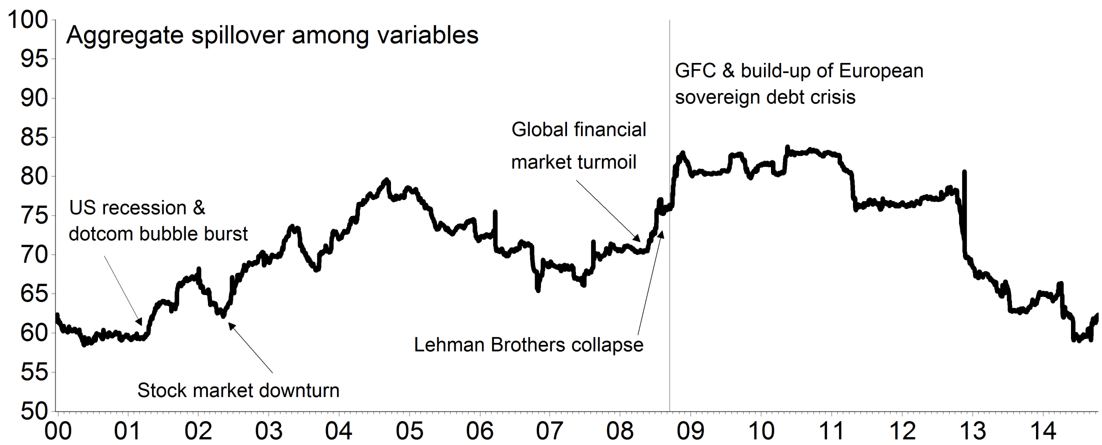

NOTE: The figure plots the aggregate spillover index obtained using a rolling window length of $w = 250$ trading days with the forecast horizon set to $h = 10$ trading days. The horizontal axis records the end date of the rolling samples. The unit of measurement is percent.

Figure 2: Time-Varying Spillover Intensity

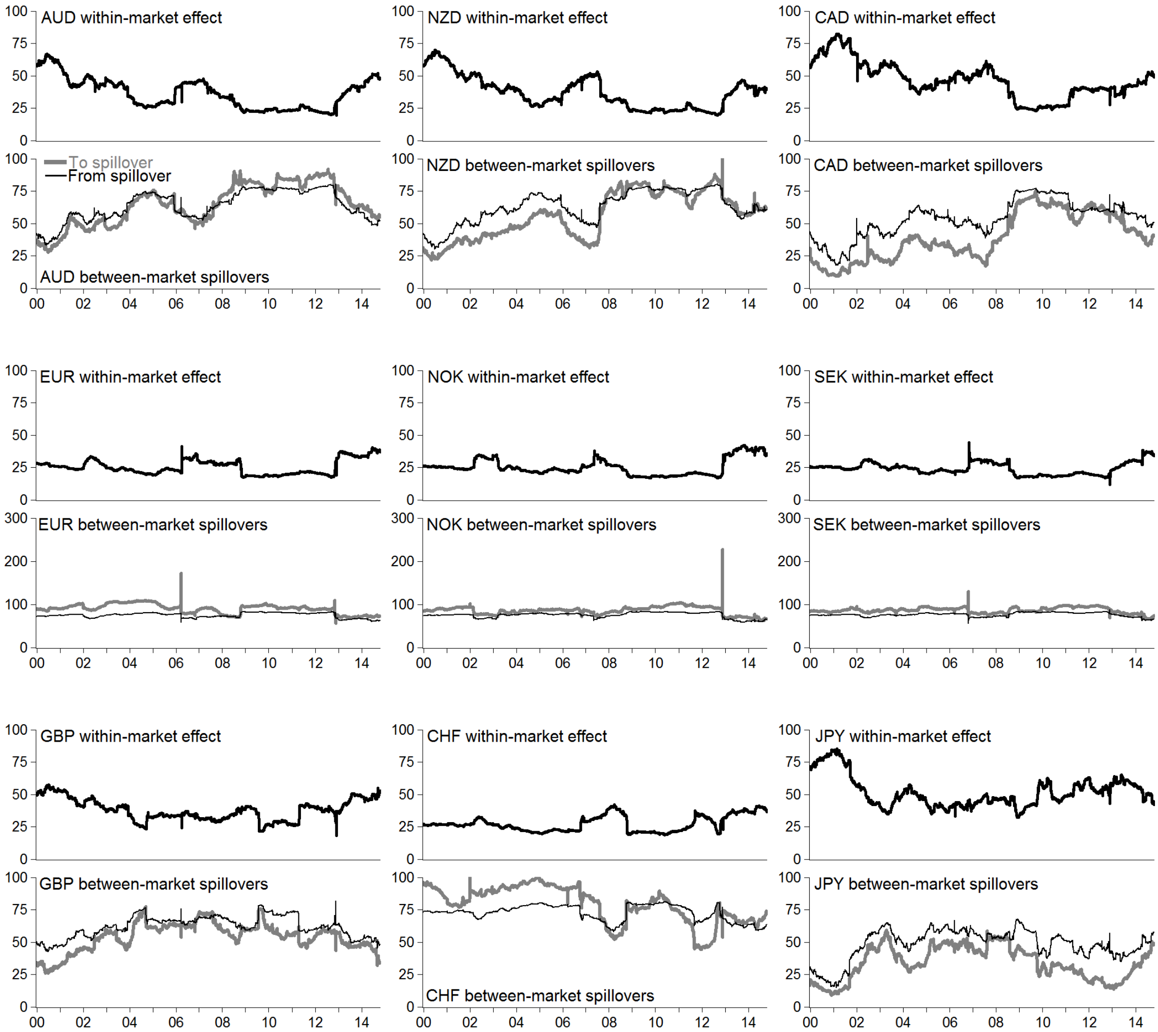

NOTE: Results are obtained using a rolling window length of $w = 250$ trading days with the forecast horizon set to $h = 10$ trading days. The horizontal axis records the end date of the rolling samples. The unit of measurement is percent. Note that the 'to spillover' may exceed 100% by virtue of its construction. The figure is laid out such that currencies which display similar behaviour appear in the same row

Figure 3: Rolling Connectedness among Markets

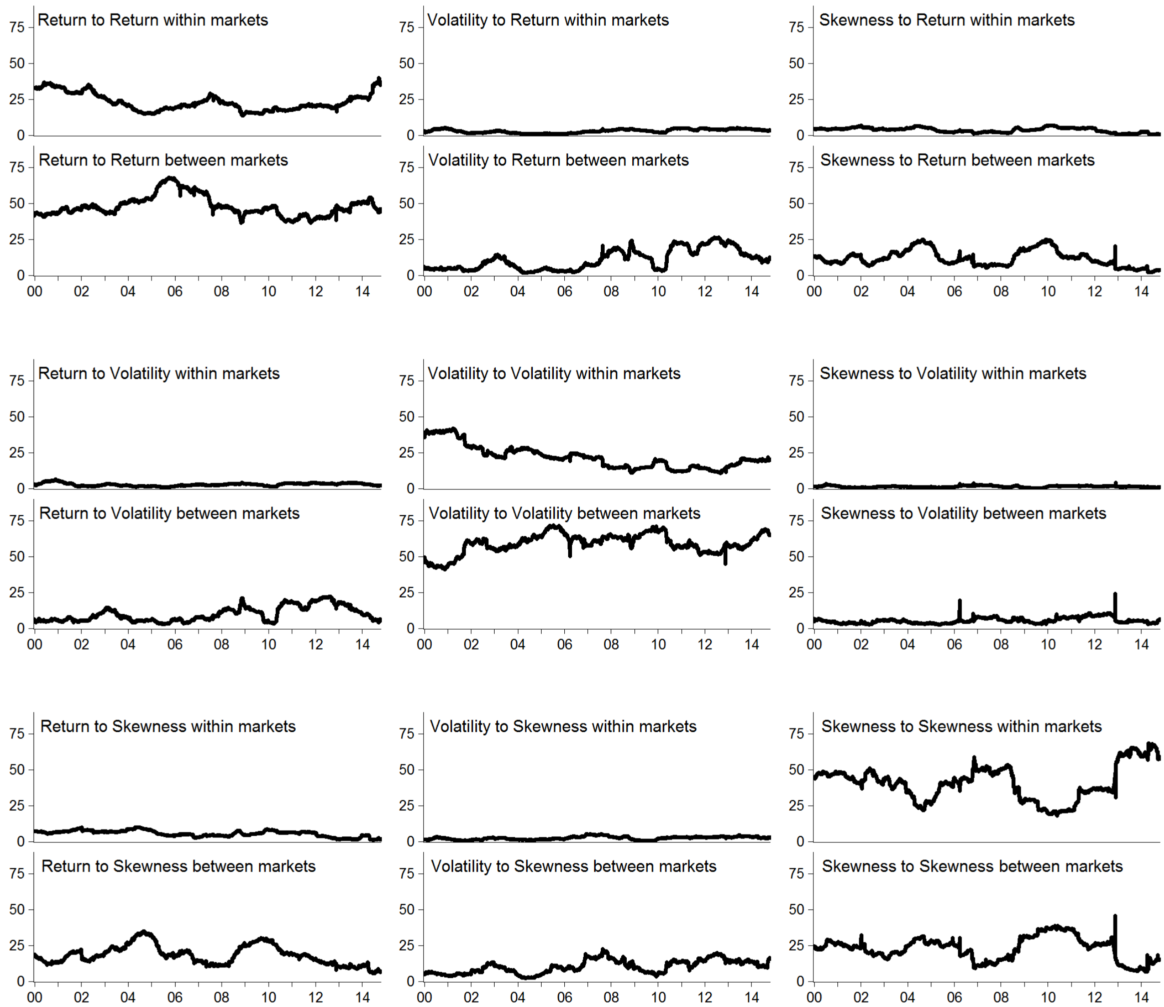

NOTE: Results are obtained using a rolling window length of $w = 250$ trading days with the forecast horizon set to $h = 10$ trading days. The horizontal axis records the end date of the rolling samples. The unit of measurement is percent. Further details of the block aggregation scheme used to compute these results may be found in the online Technical Supplement.

Figure 4: Rolling Connectedness among Moments

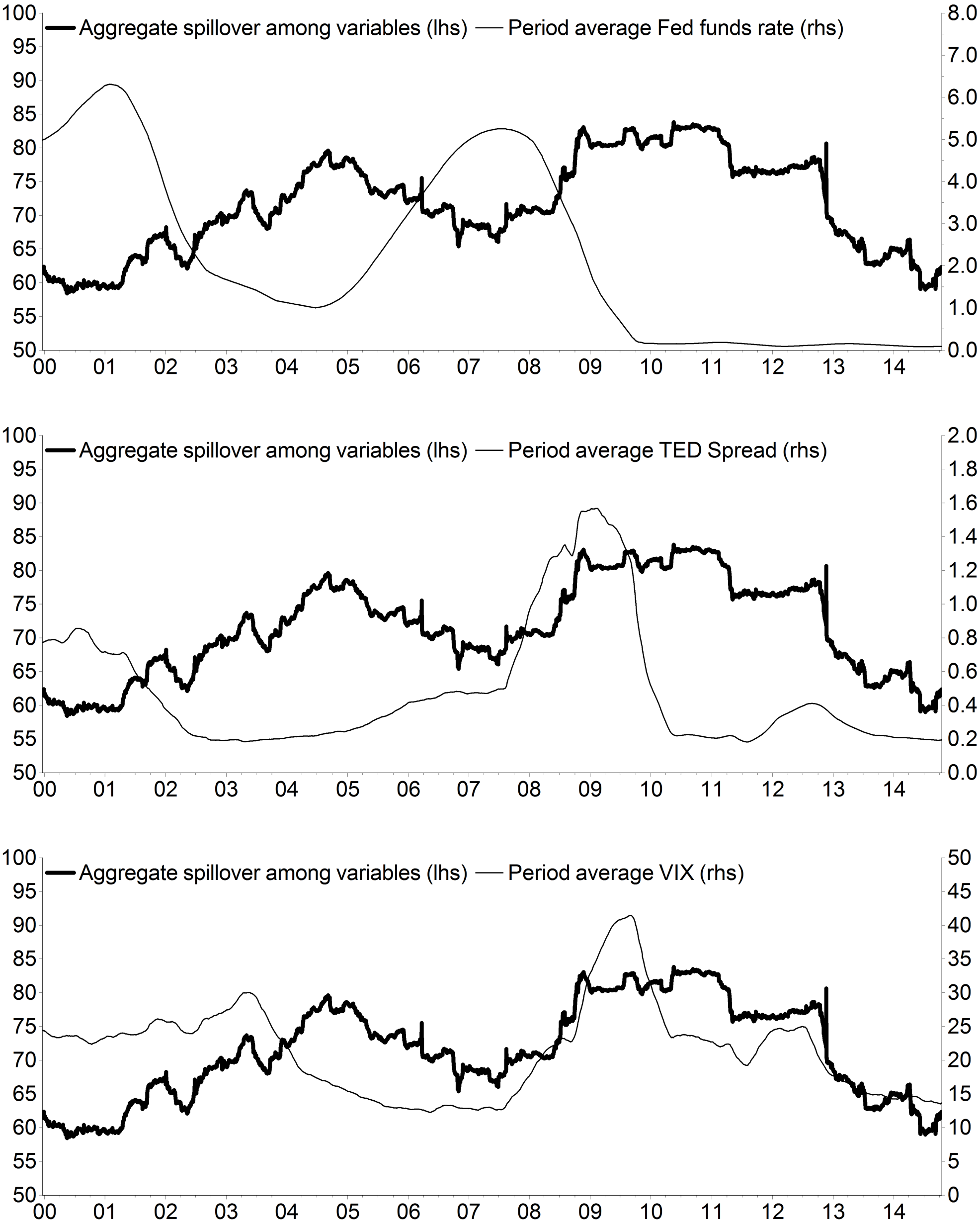

NOTE: The graphs plot the aggregate spillover index shown in Figure 2 against the period averages of the effective Federal Funds Rate, the TED spread and the VIX, respectively. The period average of the Federal funds rate at time t, for example, is computed as the mean of the effective Federal funds rate over the 250 trading days from $t - 249, \ldots, t$. This matches the data window used to compute the value of spillover index reported at time t. Data for the effective Federal Funds Rate, the TED spread and the VIX are obtained from the Federal Reserve Economic Data Service (the series IDs are 'DFF', 'TEDRATE' and 'VIXCLS', respectively).

Figure 5: Spillover Intensity versus Selected Financial Indicators

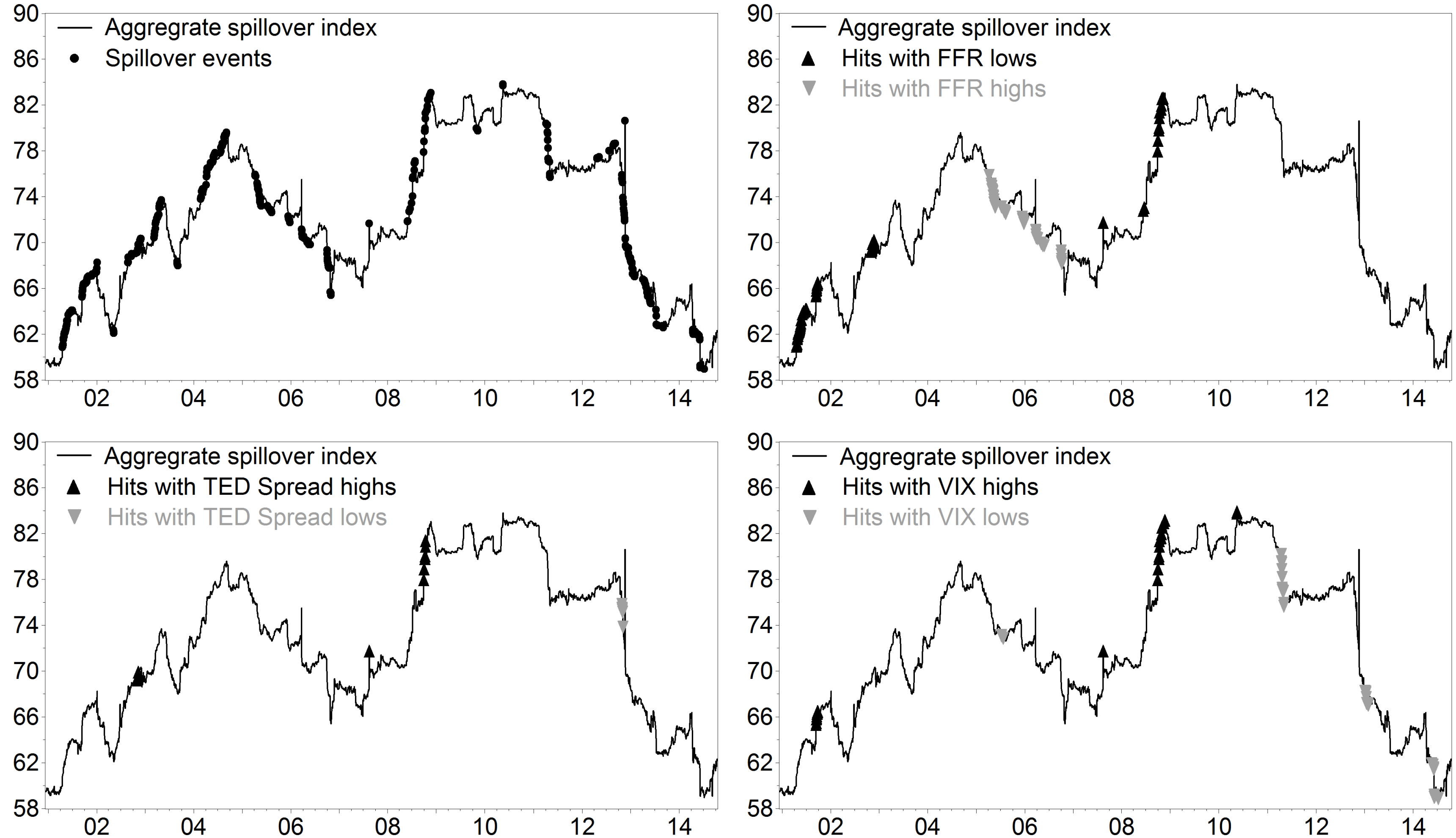

Note: In each panel, the line records the rolling aggregate spillover index as shown in Figure 2. For the reader's convenience, the upper left panel records the timing of spillover events (both new highs and new lows). In each of the remaining panels, markers identify occasions where a new 250-day high or low value of the spillover index is associated with a new 250-day high or low value of the federal funds rate, the TED spread or the VIX respectively. In the upper right panel, a black upward (gray downward) triangle indicates an occasion where the spillover index reaches a new high (low) *and* the federal funds rate reaches a new low (high) within ±5 trading days. In the two lower panels, a black upward (gray downward) triangle denotes an occasion where the spillover index reaches a new high (low) and the TED spread or the VIX, respectively, also reaches a new high (low) within ±5 trading days.

Figure 6: Analysis of the Timing of Hits

Risk and Return Spillovers among the G10 Currencies: Technical Supplement

Matthew Greenwood-Nimmo[a], Viet Hoang Nguyen[b], Barry Rafferty[a,*]

[a] *Department of Economics, University of Melbourne, 111 Barry Street, Melbourne 3053, Australia.*
[b] *Melbourne Institute of Applied Economic & Social Research, 111 Barry Street, Melbourne 3053, Australia.*

Contents

---

*Corresponding author. Tel.: +61 (0)3-8344-7198.

Email addresses: matthew.greenwood@unimelb.edu.au (Matthew Greenwood-Nimmo), vietn@unimelb.edu.au (Viet Hoang Nguyen), barry.rafferty@unimelb.edu.au (Barry Rafferty)

Version dated February 11, 2016

Appendix A. Computation of the Risk-Neutral Moments

A.1. FX Option Conventions

FX options are quoted in terms of their Garman and Kohlhagen (1983) implied volatilities. While the options are quoted in terms of their implied volatilities, the computation of the risk-neutral moments requires the actual prices of the options, since the method used is model-free. Given the implied volatilities, the actual prices of call and put options for currency i can be recovered using the Garman and Kohlhagen (1983) option pricing formulae:

$$\mathcal{C}_{it}(K_i, \tau) = e^{-r^d_{t,\tau}} \left[F^i_{t,\tau} N(d_1) - K_i N(d_2)\right] \tag{A.1}$$

$$\mathcal{P}_{it}(K_i, \tau) = e^{-r^d_{t,\tau}} \left[K_i N(-d_2) - F^i_{t,\tau} N(-d_1)\right] \tag{A.2}$$

where

$$d_1 = \frac{\ln\left(\frac{F^i_{t,\tau}}{K_i}\right) + \frac{1}{2}\sigma^2_t(K_i, \tau)\tau}{\sigma_t(K_i, \tau)\sqrt{\tau}}; \quad d_2 = d_1 - \sigma_t(K_i, \tau)\sqrt{\tau} \tag{A.3}$$

and where $\mathcal{C}_{it}(K_i, \tau)$ and $\mathcal{P}_{it}(K_i, \tau)$ are the prices of call and put options respectively for currency i, with a strike price of K_i and a maturity of τ (which is expressed as a fraction of a year). Furthermore, $F^i_{t,\tau}$ is the forward rate for currency i with maturity τ, $r^d_{t,\tau}$ is the annualised domestic interest rate (taken to be the U.S. interest rate in this paper) with maturity τ and $N(\cdot)$ is the cumulative distribution function of the standard normal distribution. Finally, $\sigma_t(K_i, \tau)$ is the volatility of exchange rate changes implied by the option pricing formula. Given an implied volatility quote and the strike price, the price of the option can therefore be easily computed.

In the over-the-counter market, implied volatility quotes for FX options are generally not given in terms of their strike prices. They are instead given for fixed option deltas. The option deltas are obtained by differentiating the value of the relevant option with respect to the spot exchange rate, S_{it}. These are given below for call and put options respectively:

$$\delta_c = e^{-r^i_{t,\tau}\tau} N(d_1) \tag{A.4}$$

$$\delta_p = -e^{-r^i_{t,\tau}\tau} N(-d_1) \tag{A.5}$$

where $r^i_{t,\tau}$ is the interest rate for currency i with maturity τ. In this paper, we determine $r^i_{t,\tau}$ using the no-arbitrage covered interest rate parity condition given by:

$$e^{r^i_{t,\tau}\tau} = e^{r^d_{t,\tau}\tau}\frac{S_{it}}{F^i_{t,\tau}} \tag{A.6}$$

Options market makers generally quote implied volatilities for portfolios of out-of-the-money (OTM) 25δ and 10δ options contracts (e.g. quotes for risk reversals and butterfly strangles) as well as an at-the-money (ATM) delta-neutral (0δ) straddle. From these, one can get implied volatility quotes for options at five different strike prices: 25δ put and call options, 10δ put and call options and ATM put and call options. With fixed deltas and implied volatility quotes, the strike prices can be backed out from the Garman and Kohlhagen (1983) formulae. The put and call strike prices with deltas of δ_c and δ_p are given by:

$$K_{i,\delta_c} = F^i_{t,\tau}\exp\left(\frac{1}{2}\sigma^2_t(\delta_c,\tau)\tau - \sigma_t(\delta_c,\tau)\sqrt{\tau}N^{-1}\left[e^{r^i_{t,\tau}\tau}\delta_c\right]\right) \tag{A.7}$$

$$K_{i,\delta_p} = F^i_{t,\tau}\exp\left(\frac{1}{2}\sigma^2_t(\delta_p,\tau)\tau + \sigma_t(\delta_p,\tau)\sqrt{\tau}N^{-1}\left[-e^{r^i_{t,\tau}\tau}\delta_p\right]\right) \tag{A.8}$$

where $N^{-1}(\cdot)$ is the inverse of the cumulative distribution function for the standard normal distribution.

Finally, we can set $\delta_{c,ATM} + \delta_{p,ATM} = 0$ and solve to get the ATM strike price for the delta-neutral straddle, which is given by:

$$K_{i,ATM} = F^i_{t,\tau}\exp\left(\frac{1}{2}\sigma^2_t(ATM,\tau)\tau\right) \tag{A.9}$$

A.2. Computing Risk-Neutral Moments from FX Options Prices

Breedon and Litzenberger (1978) were the first to show that a complete set of options on an asset allow the asset's entire risk-neutral distribution to be recovered from the options prices. If we consider an arbitrary state-contingent payoff for currency i at time $t+\tau$, that depends on the future spot rate, and denote it by $H(S_{i,t+\tau})$, it can be valued by:

$$\begin{aligned} p_{it} &= \exp(-r^d_{t,\tau})\int_0^\infty H(S_{i,t+\tau})q(S_{i,t+\tau})dS_{i,t+\tau} \\ &= \exp(-r^d_{t,\tau})E^{\mathbb{Q}}_t(H(S_{i,t+\tau})) \end{aligned} \tag{A.10}$$

where $q(S_{i,t+\tau})$ is the density of the risk-neutral distribution and $E_t^{\mathbb{Q}}(\cdot)$ is the expectation under the risk-neutral measure $\mathbb{Q}$.

In practice, we don't have a complete set of options. However, Bakshi and Madan (2000) show that any payoff with bounded expectation under the risk-neutral distribution can be spanned by a continuum of out-of-the-money put and call options. This allows the state-contingent payoff $H(S_{i,t+\tau})$ to be priced by:

$$
\begin{aligned}
p_{it} &= \exp(-r_{t,\tau}^{d})(H(\bar{S}_i) - \bar{S}_i) + H_S(\bar{S}_i)S_{it} \\
&+ \int_0^{\bar{S}_i} H_{SS}(K_i)\mathcal{P}_{it}(K_i,\tau)dK_i + \int_{\bar{S}_i}^{\infty} H_{SS}(K_i)\mathcal{C}_{it}(K_i,\tau)dK_i
\end{aligned} \tag{A.11}
$$

where K_i are option strike prices, H_S and H_{SS} are the first and second derivatives of the state-contingent payoff function and $\mathcal{C}_{it}(K_i,\tau)$ and $\mathcal{P}_{it}(K_i,\tau)$ are the prices of call and put options with a strike price of K_i and maturity of τ. $\bar{S}_i$ is a future value of the spot exchange rate for currency i, typically taken to be equal to the forward rate $F_{t,\tau}^{i}$.

Bakshi et al. (2003) show that if we set $H(S_{i,t+\tau}) = (\ln(S_{i,t+\tau}) - \ln(S_{it}))^n$, the values of the discounted non-central moments of the risk-neutral distribution can be valued by Equation (A.11). The discounted non-central second, third and fourth moments of the risk-neutral distribution of exchange rate changes for currency i are denoted by $V_{it}(\tau)$, $W_{it}(\tau)$ and $X_{it}(\tau)$ respectively and are given by:

$$
\begin{aligned}
V_{it}(\tau) &= \int_{\bar{S}_i}^{\infty} \frac{2\left(1 - \ln\left(\frac{K_i}{\bar{S}_i}\right)\right)}{K_i^2}\mathcal{C}_{it}(K_i,\tau)dK_i \\
&+ \int_0^{\bar{S}_i} \frac{2\left(1 + \ln\left(\frac{\bar{S}_i}{K_i}\right)\right)}{K_i^2}\mathcal{P}_{it}(K_i,\tau)dK_i
\end{aligned} \tag{A.12}
$$

$$
\begin{aligned}
W_{it}(\tau) &= \int_{\bar{S}_i}^{\infty} \frac{6\ln\left(\frac{K_i}{\bar{S}_i}\right) - 3\left(\ln\left(\frac{K_i}{\bar{S}_i}\right)\right)^2}{K_i^2}\mathcal{C}_{it}(K_i,\tau)dK_i \\
&- \int_0^{\bar{S}_i} \frac{6\ln\left(\frac{\bar{S}_i}{K_i}\right) + 3\left(\ln\left(\frac{\bar{S}_i}{K_i}\right)\right)^2}{K_i^2}\mathcal{P}_{it}(K_i,\tau)dK_i
\end{aligned} \tag{A.13}
$$

$$X_{it}(\tau) = \int_{\bar{S}_i}^{\infty} \frac{12\left(\ln\left(\frac{K_i}{\bar{S}_i}\right)\right)^2 - 4\left(\ln\left(\frac{K_i}{\bar{S}_i}\right)\right)^3}{K_i^2} \mathcal{C}_{it}(K_i,\tau)dK_i$$

$$+ \int_{0}^{\bar{S}_i} \frac{12\left(\ln\left(\frac{\bar{S}_i}{K_i}\right)\right)^2 + 4\left(\ln\left(\frac{\bar{S}_i}{K_i}\right)\right)^3}{K_i^2} \mathcal{P}_{it}(K_i,\tau)dK_i \tag{A.14}$$

Using these and doing some transformations gives the risk-neutral volatility, risk-neutral skewness and risk-neutral kurtosis, which are given by:

$$\text{VOL}_{it}^{RN}(\tau) = \left[e^{r_{t,\tau}^d \tau} V_{it}(\tau) - \mu_{it}(\tau)^2\right]^{\frac{1}{2}} \tag{A.15}$$

$$\text{SKEW}_{it}^{RN}(\tau) = \frac{e^{r_{t,\tau}^d \tau} W_{it}(\tau) - 3\mu_{it}(\tau) e^{r_{t,\tau}^d \tau} V_{it}(\tau) + 2\mu_{it}(\tau)^3}{\left[e^{r_{t,\tau}^d \tau} V_{it}(\tau) - \mu_{it}(\tau)^2\right]^{\frac{3}{2}}} \tag{A.16}$$

$$\text{KURT}_{it}^{RN}(\tau) = \frac{e^{r_{t,\tau}^d \tau} X_{it}(\tau) - 4\mu_{it}(\tau) e^{r_{t,\tau}^d \tau} W_{it}(\tau) + 6\mu_{it}(\tau)^2 e^{r_{t,\tau}^d \tau} V_{it}(\tau) - 3\mu_{it}(\tau)^4}{\left[e^{r_{t,\tau}^d \tau} V_{it}(\tau) - \mu_{it}(\tau)^2\right]^{2}} \tag{A.17}$$

where the mean of the risk-neutral distribution is given by:

$$\mu_{it}(\tau) = e^{(r_{t,\tau}^d - r_{t,\tau}^i)\tau} - 1 - e^{r_{t,\tau}^d \tau} \left(\frac{V_{it}(\tau)}{2} + \frac{W_{it}(\tau)}{6} + \frac{X_{it}(\tau)}{24}\right) \tag{A.18}$$

To compute these risk-neutral moments requires a continuum of out-of-the-money call and put options. In practice though, there is only a limited range of strikes at which options are quoted. However, Jiang and Tian (2005) argue based on sensitivity results that the available cross section of foreign exchange options is sufficient, when combined with interpolation, to ensure the errors in extracting the risk-neutral moments are very small. To interpolate the implied volatility function, we use the vanna-volga method (see Castagna and Mercurio, 2007). In addition, we extrapolate the implied volatility functions by appending flat tails.

Appendix B. Further Information about the Dataset

The sample used in estimation covers the period 31-Dec-1998 to 14-Oct-2014 at daily frequency. Prior to any subsequent manipulations, all non-trading days are removed from the sample. The return series for the ith currency is then constructed as the log-difference of the relevant spot exchange rate against the U.S. dollar.

The construction of the risk-neutral moments is detailed in Appendix A above. The innovations to the risk-neutral moments are constructed as the residuals from an auxiliary $AR(1)$ regression on the time series of the risk-neutral moments over the full sample period, as documented in Section 3 of the paper.

The three macroeconomic and financial series used in Section 6 of the paper were downloaded at daily frequency from the Federal Reserve Economic Data Service. Their dates were first matched against those of the returns and the risk-neutral moments and then the required moving averages were computed over rolling samples of 250 trading days as described in the notes to Figure 5.

Table B.1 provides basic summary statistics for the FX data used in estimation (summary statistics for the macro-financial series are available on request). All currencies in our sample except the GBP appreciated against the U.S. dollar during our sample, with the annualised rate of return over the full sample varying between -0.03% (GBP) and 2.4% (NZD). The standard deviation of the RNV innovations is largest for those currencies which are closely linked by carry trades, notably the JPY and AUD. Meanwhile, the GBP and the CAD are notable for the high degree of time variation in their RNS innovations.

Figures B.1–B.3 provide time series plots of the data. These reveal considerable commonality in the evolution of spot exchange rates for the European currencies reflecting their exposure to common influences. A marked spike in RNV is observed across all markets in September 2008 following the collapse of Lehman Brothers and a pronounced increase in the magnitude and volatility of RNS innovations is evident in many markets thereafter.

		AUD	CAD	EUR	JPY	NZD	NOK	SEK	CHF	GBP
Spot Rate	Mean	0.783	0.840	1.225	0.010	0.657	0.152	0.133	0.852	1.662
	Std Dev	0.168	0.136	0.183	0.001	0.136	0.023	0.019	0.178	0.169
Annualised Return	Mean	0.022	0.019	0.005	0.003	0.024	0.009	0.007	0.022	-0.003
	Std Dev	0.131	0.091	0.099	0.103	0.135	0.119	0.120	0.107	0.091
RNV	Mean	0.122	0.090	0.106	0.111	0.133	0.121	0.123	0.109	0.093
	Std Dev	0.048	0.035	0.033	0.034	0.042	0.037	0.038	0.028	0.033
RNV Innovations	Mean	0.000	0.000	0.000	0.000	0.000	0.000	0.000	0.000	0.000
	Std Dev	0.006	0.004	0.004	0.006	0.006	0.004	0.004	0.005	0.004
RNS	Mean	-0.193	-0.478	-0.232	0.050	-0.122	-0.078	-0.169	-0.260	-0.303
	Std Dev	0.334	0.477	0.428	0.445	0.292	0.277	0.240	0.359	0.448
RNS Innovations	Mean	0.000	0.000	0.000	0.000	0.000	0.000	0.000	0.000	0.000
	Std Dev	0.087	0.118	0.092	0.118	0.061	0.076	0.081	0.113	0.149

NOTES: The spot rate is the exchange rate of each currency in units of foreign currency per U.S. dollar. Daily returns are given by the daily log change in the spot exchange rate. Although daily returns are used in estimation, statistics for the annualised returns are reported here for ease of interpretation. RNV and RNS refer to the risk-neutral volatility and risk-neutral skewness (respectively) for each currency extracted from the FX options data. Following Menkhoff et al. (2012) and Chang et al. (2013), the innovations in RNV and RNS are recovered as the residuals from auxiliary AR(1) models as documented in Section 3 of the paper.

Table B.1: Full-Sample Descriptive Statistics

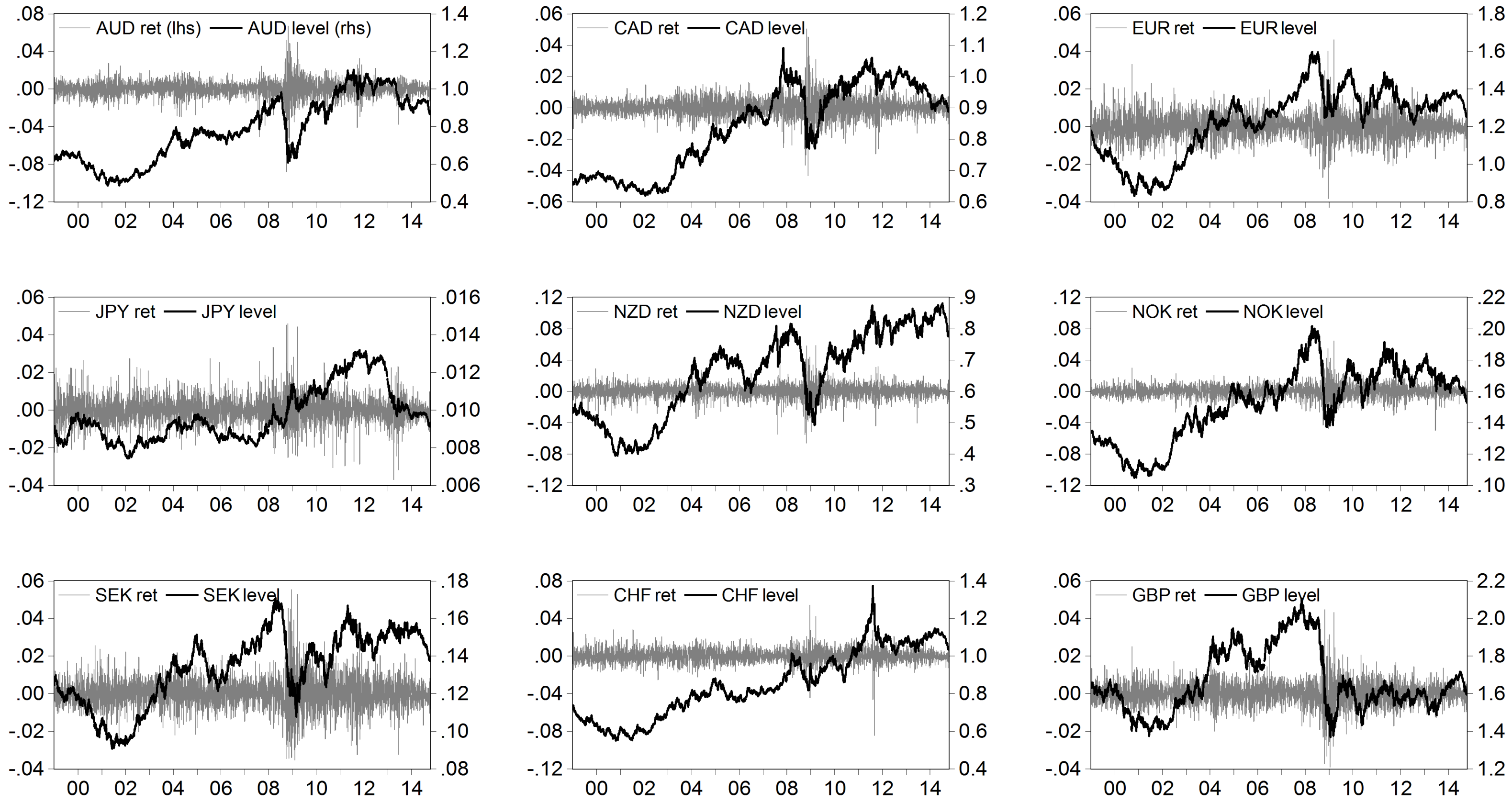

Figure B.1: Spot Exchange Rates and Daily Returns by Market

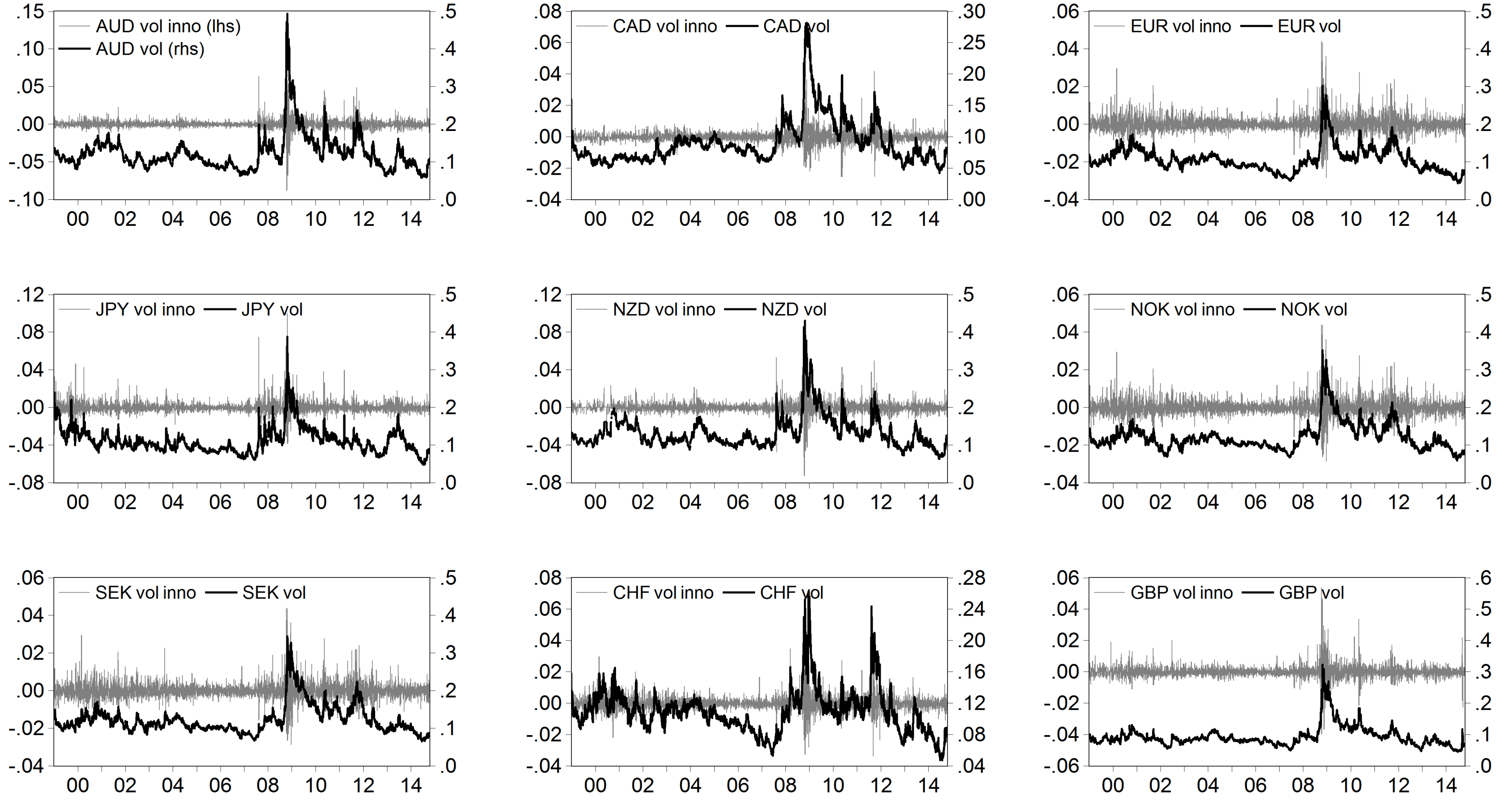

NOTE: The RNV innovations are computed as the residuals from an AR(1) process following the approach adopted by Menkhoff et al. (2012).

Figure B.2: Level and Innovations of Risk-Neutral Volatility (RNV) by Market

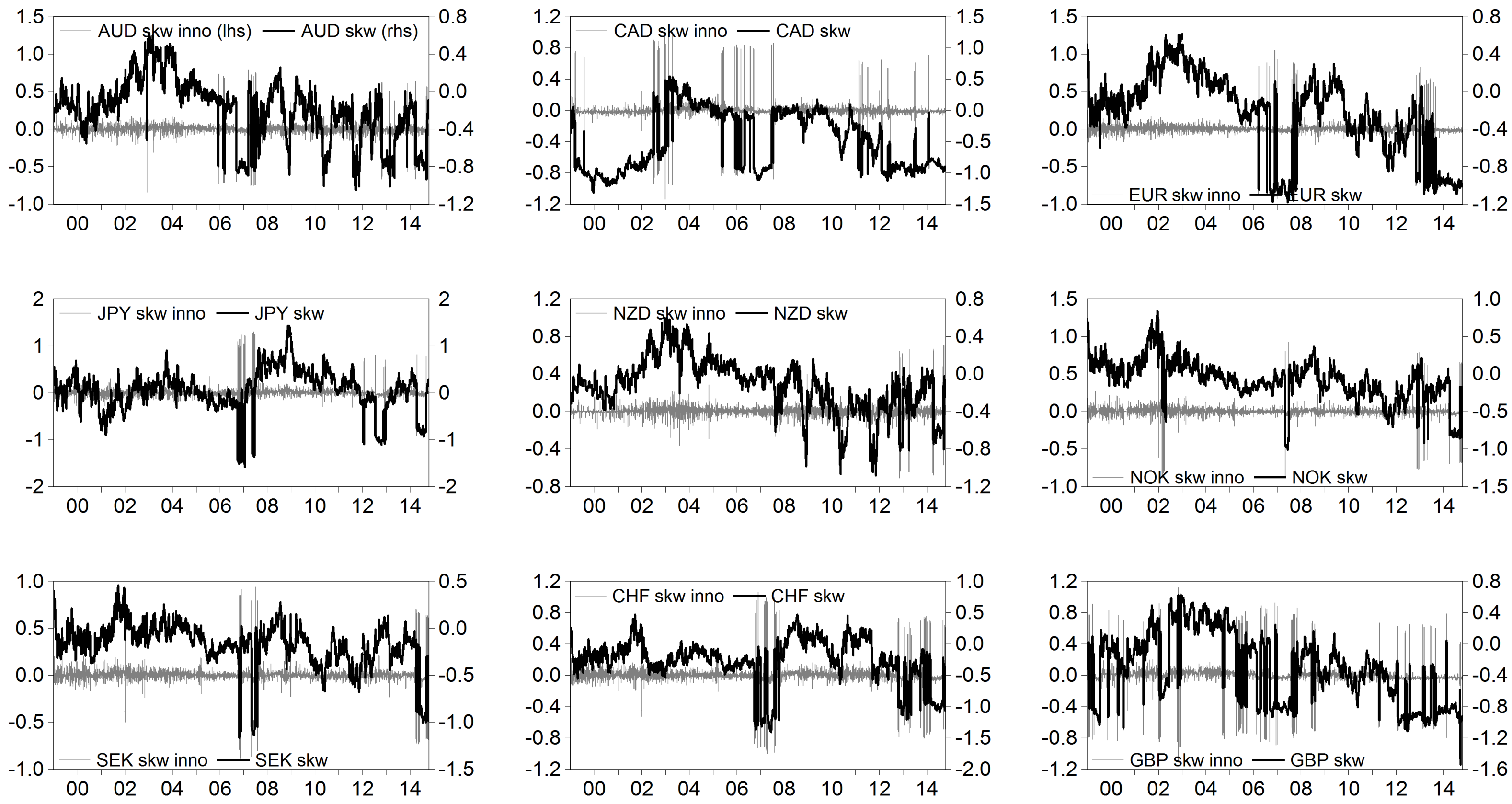

NOTE: The RNS innovations are computed as the residuals from an AR(1) process following the approach adopted by Chang et al. (2013).

Figure B.3: Level and Innovations of Risk-Neutral Skewness (RNS) by Market

Appendix C. Aggregation into Moment Groups

To evaluate the connectedness among the three groups of moments — r, v and s — for all N markets collectively, one simply reorders the variables in the VAR to obtain $\mathbf{y}_t = (\mathbf{r}_t, \mathbf{v}_t, \mathbf{s}_t)'$ where $\mathbf{r}_t = (r_{1t}, r_{2t}, \ldots, r_{Nt})'$, $\mathbf{v}_t = (v_{1t}, v_{2t}, \ldots, v_{Nt})'$ and $\mathbf{s}_t = (s_{1t}, s_{2t}, \ldots, s_{Nt})'$. In this case, we may write the h-step-ahead connectedness matrix as follows:

$$\mathbb{C}^{(h)} = \begin{bmatrix} \mathbf{B}^{(h)}_{r\leftarrow r} & \mathbf{B}^{(h)}_{r\leftarrow v} & \mathbf{B}^{(h)}_{r\leftarrow s} \\ \mathbf{B}^{(h)}_{v\leftarrow r} & \mathbf{B}^{(h)}_{v\leftarrow v} & \mathbf{B}^{(h)}_{v\leftarrow s} \\ \mathbf{B}^{(h)}_{s\leftarrow r} & \mathbf{B}^{(h)}_{s\leftarrow v} & \mathbf{B}^{(h)}_{s\leftarrow s} \end{bmatrix} \tag{C.1}$$

where we aggregate into $g = 3$ groups (i.e. r, v and s) each composed of $m = N$ variables:

$$\mathbf{B}^{(h)}_{r\leftarrow r} = \begin{bmatrix} \theta^{(h)}_{r_1\leftarrow r_1} & \theta^{(h)}_{r_1\leftarrow r_2} & \ldots & \theta^{(h)}_{r_1\leftarrow r_N} \\ \theta^{(h)}_{r_2\leftarrow r_1} & \theta^{(h)}_{r_2\leftarrow r_2} & \ldots & \theta^{(h)}_{r_2\leftarrow r_N} \\ \vdots & \vdots & \ddots & \vdots \\ \theta^{(h)}_{r_N\leftarrow r_1} & \theta^{(h)}_{r_N\leftarrow r_2} & \ldots & \theta^{(h)}_{r_N\leftarrow r_N} \end{bmatrix}, \quad \mathbf{B}^{(h)}_{r\leftarrow v} = \begin{bmatrix} \theta^{(h)}_{r_1\leftarrow v_1} & \theta^{(h)}_{r_1\leftarrow v_2} & \ldots & \theta^{(h)}_{r_1\leftarrow v_N} \\ \theta^{(h)}_{r_2\leftarrow v_1} & \theta^{(h)}_{r_2\leftarrow v_2} & \ldots & \theta^{(h)}_{r_2\leftarrow v_N} \\ \vdots & \vdots & \ddots & \vdots \\ \theta^{(h)}_{r_N\leftarrow v_1} & \theta^{(h)}_{r_N\leftarrow v_2} & \ldots & \theta^{(h)}_{r_N\leftarrow v_N} \end{bmatrix}$$

and likewise for the remaining blocks. Block connectedness measures can be computed at the level of the three groups of moments based on (C.1) following the method described in Section 2.3 of the paper.

The values shown in Figure 4 of the paper are computed from (C.1) over rolling samples. To see this, it is sufficient to consider the leftmost and central panels in the top row of Figure 4, which correspond to the blocks $\mathbf{B}^{(h)}_{r\leftarrow r}$ and $\mathbf{B}^{(h)}_{r\leftarrow v}$ in (C.1). First, 'Return to Return within markets' is computed as:

$$\mathcal{W}^{(h)}_{r\leftarrow r} = \frac{1}{m}\text{trace}\left(\mathbf{B}^{(h)}_{r\leftarrow r}\right) \tag{C.2}$$

while 'Return to Return between markets' is given by:

$$\mathcal{F}^{(h)}_{r\leftarrow r} = \frac{1}{m}\mathbf{e}'_m \mathbf{B}^{(h)}_{r\leftarrow r}\mathbf{e}_m - \mathcal{W}^{(h)}_{r\leftarrow r}. \tag{C.3}$$

Similarly, 'Volatility to Return within markets' is computed as follows:

$$\mathcal{W}^{(h)}_{r\leftarrow v} = \frac{1}{m}\text{trace}\left(\mathbf{B}^{(h)}_{r\leftarrow v}\right) \tag{C.4}$$

while 'Volatility to Return between markets' is defined by:

$$\mathcal{F}^{(h)}_{r\leftarrow v} = \frac{1}{m}\mathbf{e}'_m \mathbf{B}^{(h)}_{r\leftarrow v}\mathbf{e}_m - \mathcal{W}^{(h)}_{r\leftarrow v}. \tag{C.5}$$

The extension to the remaining panels of Figure 4 is straightforward.

Appendix D. Robustness to the Inclusion of Risk-Neutral Kurtosis

To verify that the exclusion of the risk-neutral kurtosis (RNK) from the model does not materially affect our results, we re-estimate the system including returns, RNV innovations, RNS innovations and RNK innovations for the same group of markets over the same sample period. We then repeat our analysis and find that the results under each setting are qualitatively similar. An illustration of this similarity is provided in Figure D.1 below, which recreates Figure 2 from the paper for the cases with and without kurtosis.

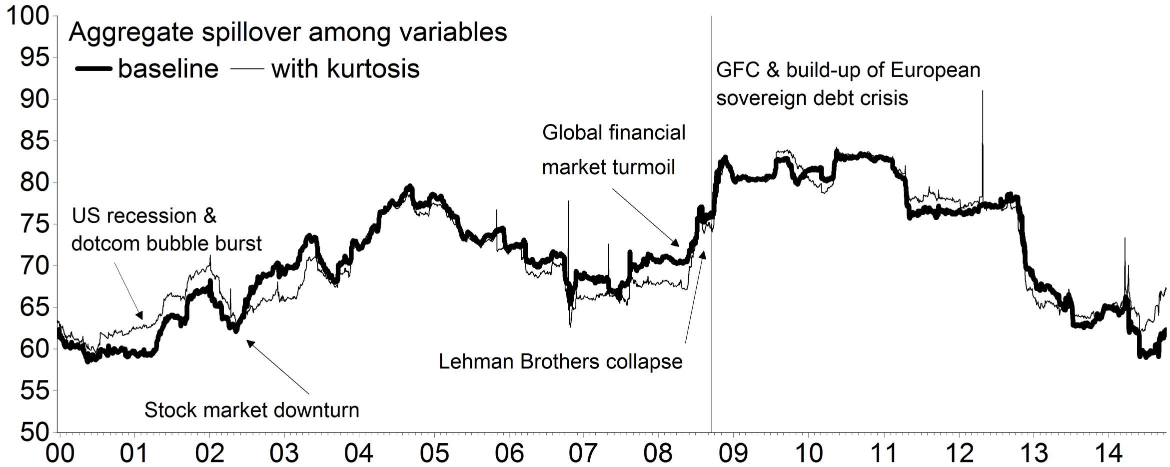

Note: In each panel, the heavy line corresponds to our baseline result (excluding RNK) while the fine line corresponds to the result from a system including RNK.

Figure D.1: Robustness of the Spillover Index, with and without Kurtosis

Table D.1 shows that the spillover indices with and without kurtosis comove closely, so the inclusion of kurtosis within the system does not yield much additional information.

	Spillover among variables
Correlation Coefficient	0.96
Directional Similarity	0.76

Note: The directional similarity measure records the proportion of periods in which our baseline spillover index moves in the same direction as the alternative version including kurtosis.

Table D.1: Comovement of Spillover Indices, with and without Kurtosis

Appendix E. High Resolution Colour Versions of Figure 6

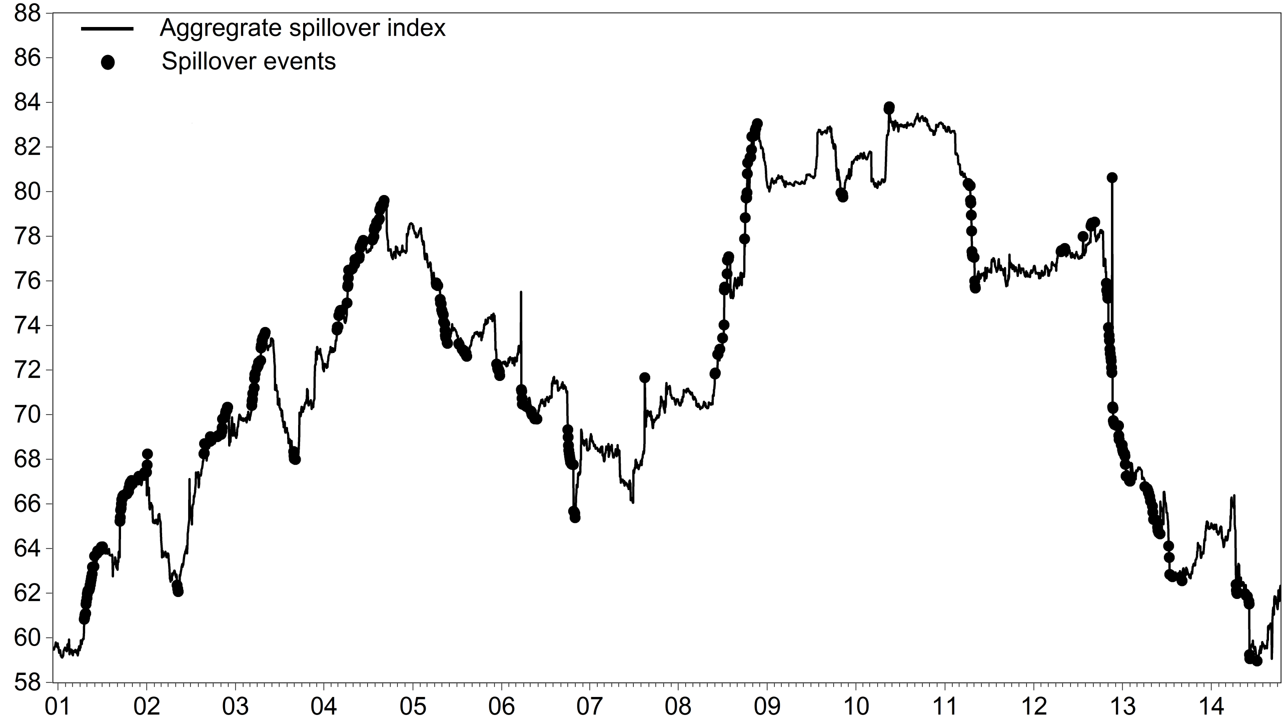

Note: This figure reproduces the information in the upper left panel of Figure 6 in the paper. The line records the rolling aggregate spillover index while the dots record the timing of spillover events (both new highs and new lows) identified following the discussion in Section 6 of the paper.

Figure E.1: Timing of Spillover Events (250-day Highs and Lows)

NOTE: This figure reproduces the information in the upper right panel of Figure 6 in the paper. The line records the rolling aggregate spillover index. A blue upward (red downward) triangle indicates an occasion where the spillover index reaches a new high (low) *and* the federal funds rate reaches a new low (high) within ±5 trading days.

Figure E.2: Timing of Hits with the Federal Funds Rate

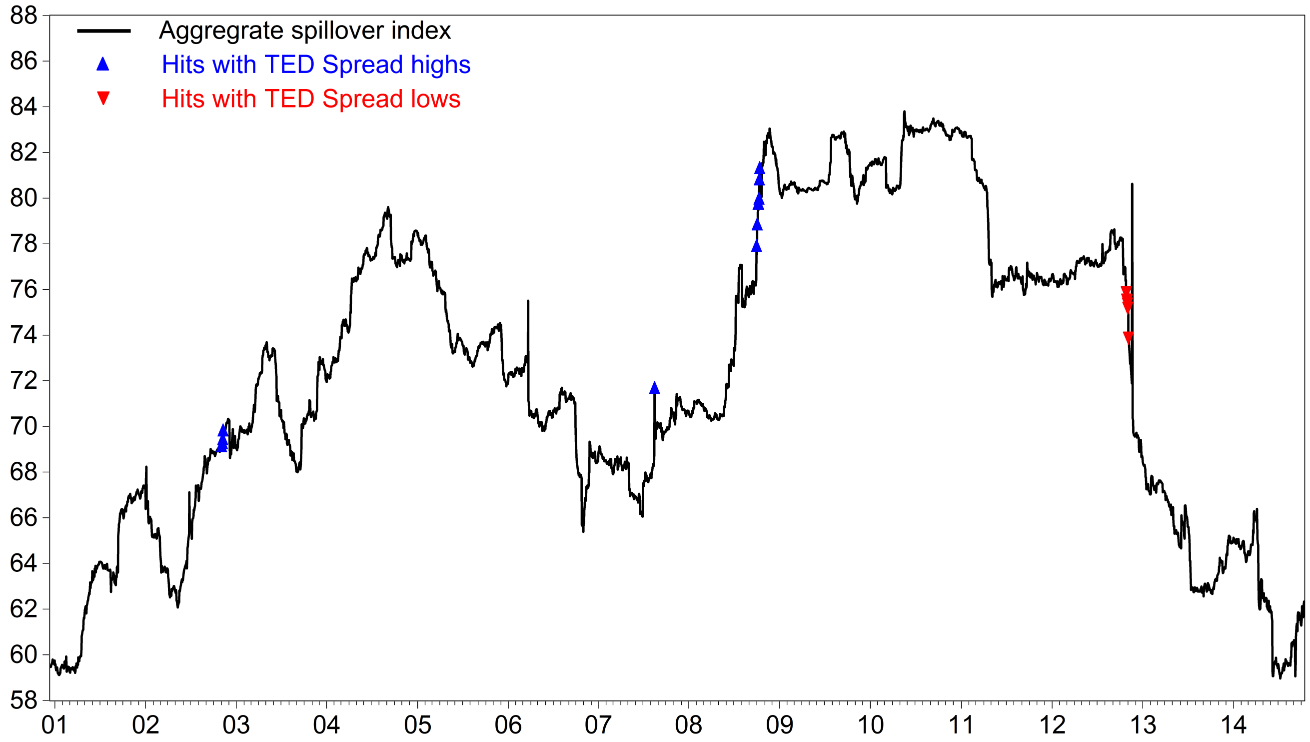

NOTE: This figure reproduces the information in the lower left panel of Figure 6 in the paper. The line records the rolling aggregate spillover index. A blue upward (red downward) triangle indicates an occasion where the spillover index reaches a new high (low) *and* the TED spread also reaches a new high (low) within ± 5 trading days.

Figure E.3: Timing of Hits with the TED Spread

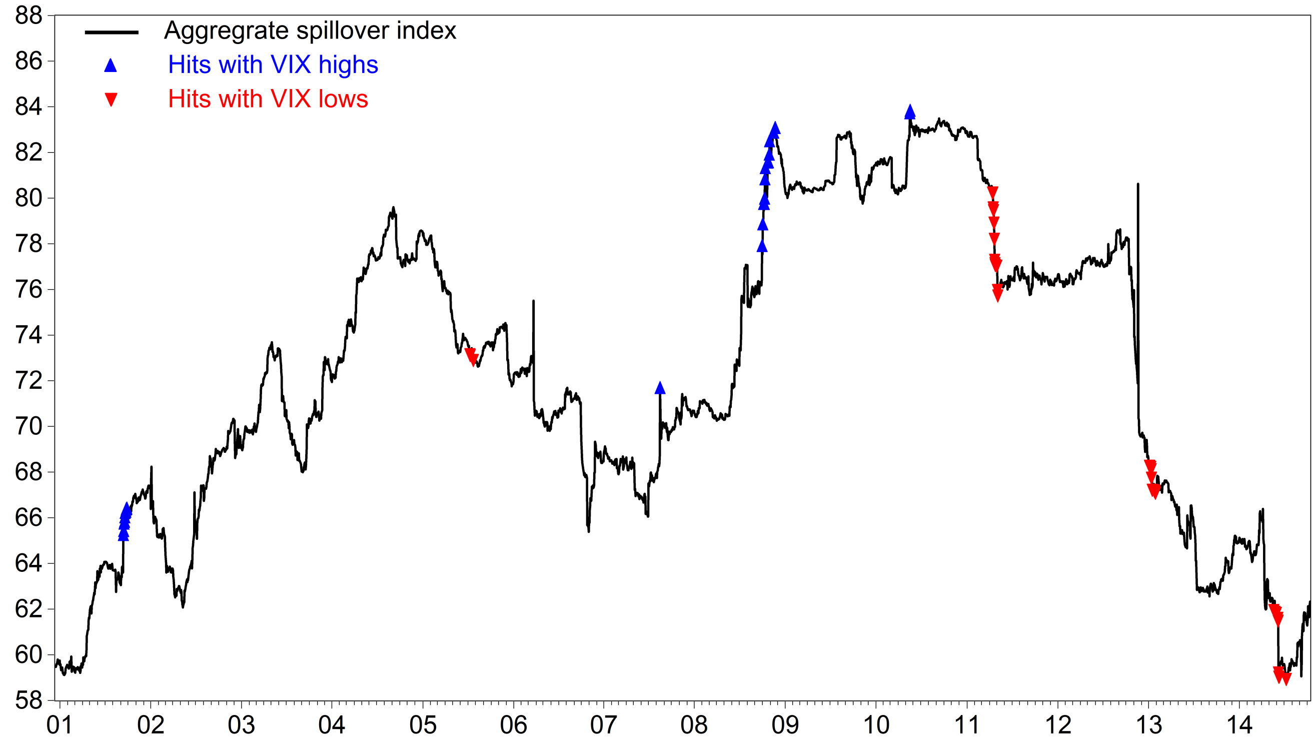

NOTE: This figure reproduces the information in the lower right panel of Figure 6 in the paper. The line records the rolling aggregate spillover index. A blue upward (red downward) triangle indicates an occasion where the spillover index reaches a new high (low) *and* the VIX also reaches a new high (low) within ±5 trading days.

Figure E.4: Timing of Hits with the VIX

References

Bakshi, G., Kapadia, N., Madan, D., 2003. Stock Return Characteristics, Skew Laws and the Differential Pricing of Individual Equity Options. Review of Financial Studies 16, 101–143.

Bakshi, G., Madan, D., 2000. Spanning and Derivative-Security Valuation. Journal of Financial Economics 55, 205–238.

Breedon, D., Litzenberger, R., 1978. Prices of State-Contingent Claims Implicit in Option Prices. Journal of Business, 617–651.

Castagna, A., Mercurio, F., 2007. The Vanna-Volga Method for Implied Volatilities. Risk 20, 106–111.

Chang, B. Y., Christoffersen, P., Jacobs, K., 2013. Market Skewness Risk and the Cross-Section of Stock Returns. Journal of Financial Economics 107, 46–68.

Garman, M. B., Kohlhagen, S. W., 1983. Foreign Currency Option Values. Journal of International Money and Finance 2, 231–237.

Jiang, G. J., Tian, Y. S., 2005. The Model-Free Implied Volatility and its Information Content. Review of Financial Studies 18, 1305–1342.

Menkhoff, L., Sarno, L., Schmeling, M., Schrimpf, A., 2012. Carry Trades and Global Foreign Exchange Volatility. The Journal of Finance 67, 681–718.